Facile grinding method synthesis of SnS_2@HKUST-1 and SnS_2@Ni-MOF for Electrocatalytic Hydrogen Evolution

Hongtao Cui, Lige Gong, Hongyan Lv, Limin Dong,* Jihua Wang, Jingyu Zhang, Yitong Mu, Yunhao Gu, Hui Li, Binghe Yang, Meijia Wang

School of Materials Science and Chemical Engineering, Harbin University of Science and Technology, Harbin 150080, China,E-mail:donglm@hrbust.edu.cn

1.1 Synthesis of different SnS_2

Synthesis of different S1: Sulfourea (0.304 g, 4 mmol) was dissolved in 40 mL distilled water and added with stirring to $SnCl_4$ (1.042 g, 4 mmol) for 30min. Then, this solution was sealed in a 100mL Teflon-lined steel autoclave, heated at 180°C for 12h and then cooled to room temperature. The yellow powder(**S1**) was separated by filtration, washed with distilled water and dried in air.

Synthesis of different S2: The synthetic procedure of **S2** was identical to **S1**, except using Thioacetamide (TAA, 0.305 g, 4 mmol) instead of Sulfourea.

Synthesis of different S3: The synthetic procedure of **S3** was identical to **S1**, except and the pH value was adjusted to 8.5 by 1 M NaOH.

Synthesis of different S4: The synthetic procedure of **S4** was identical to **S3**, except using Thioacetamide (TAA, 0.305 g, 4 mmol) instead of Sulfourea.

Synthesis of different S5: The synthetic procedure of **S5** was identical to **S1**, except using $C_8H_{12}O_8Sn$ (Tin(IV) acetate, 0.174 g, 4 mmol) instead of $SnCl_4$.

Synthesis of different S6: The synthetic procedure of **S6** was identical to **S5**, except using Thioacetamide (TAA, 0.305 g, 4 mmol) instead of Sulfourea.

Synthesis of different S7: The synthetic procedure of **S7** was identical to **S5**, except and the pH value was adjusted to 8.5 by 1 M NaOH.

The formula for calculating Rct:

$$\boldsymbol{Z = R_e + \frac{1}{j\omega C_d + \frac{1}{R_{ct} + \sigma\omega^{-1/2}(1-j)}}} \qquad (1)$$

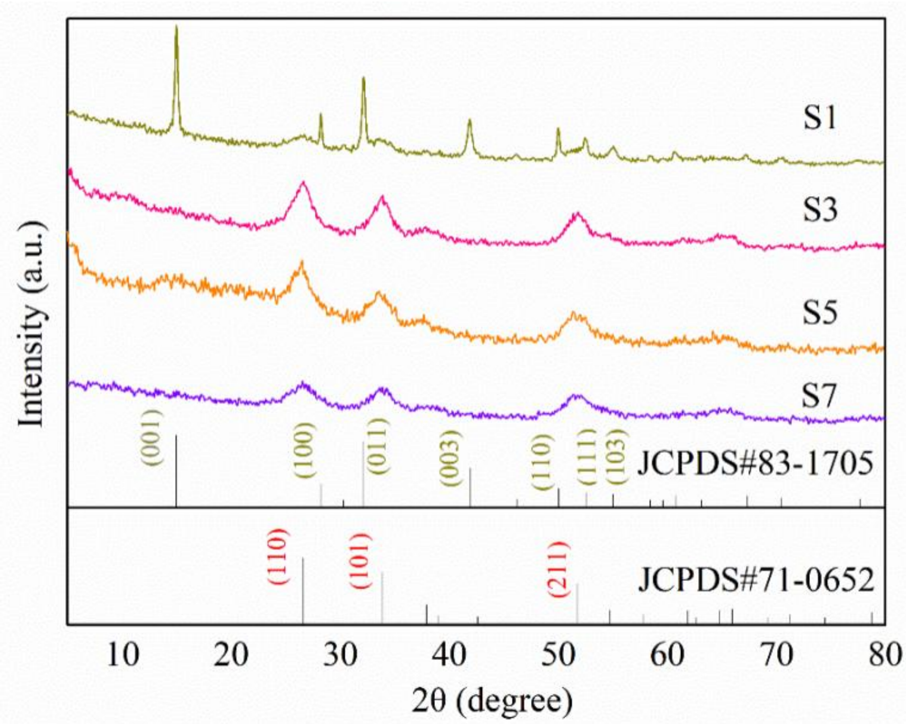

Figure SI1 The XRD patterns of the S1, S3, S5, and S7 samples.

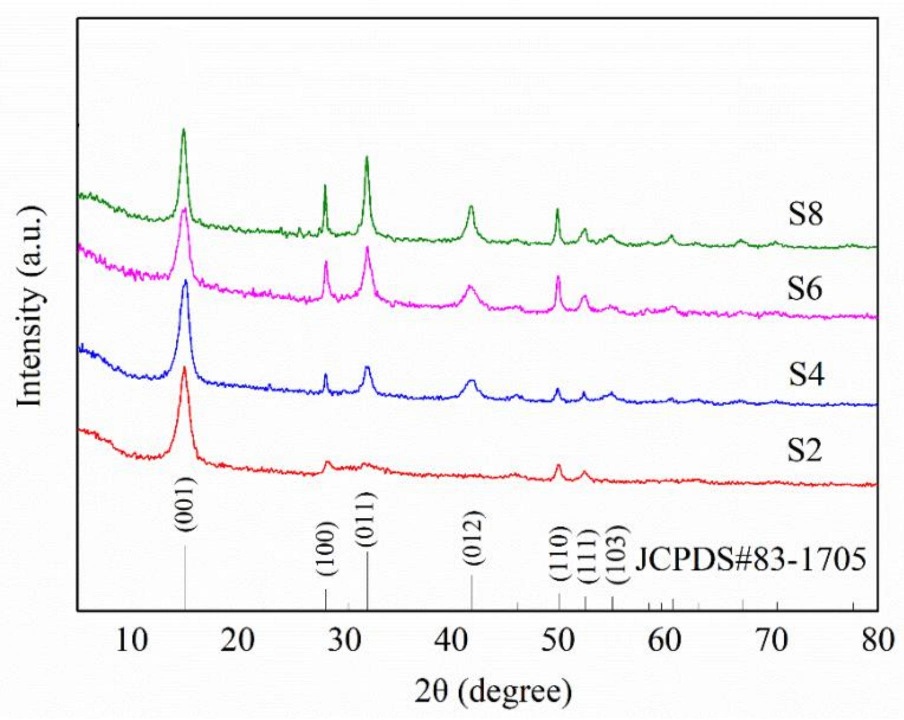

Figure SI2 The XRD patterns of the S2, S4, S6 and S8 samples.

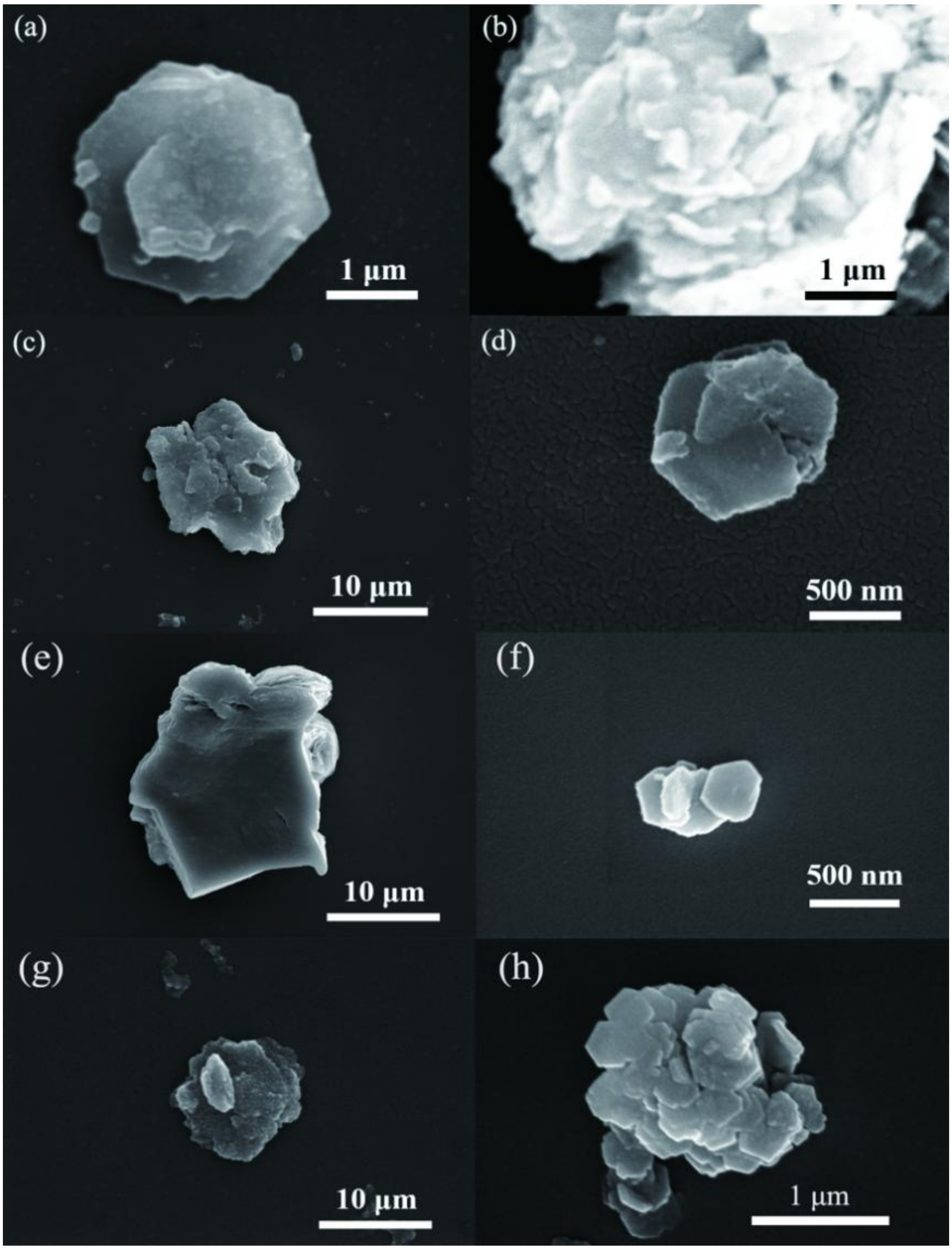

Figure SI3 (a) SEM diagram of **S1**,(b) SEM diagram of **S2**,(c) SEM diagram of **S3**,(d) SEM diagram of **S4**,(e) SEM diagram of **S5**,(f) SEM diagram of **S6**,(g) SEM diagram of **S7**,(h) SEM diagram of **S8.**

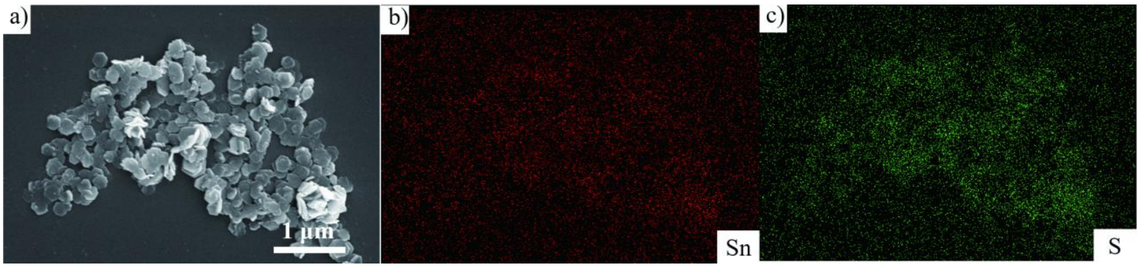

Figure SI4 the EDS of **S8**.

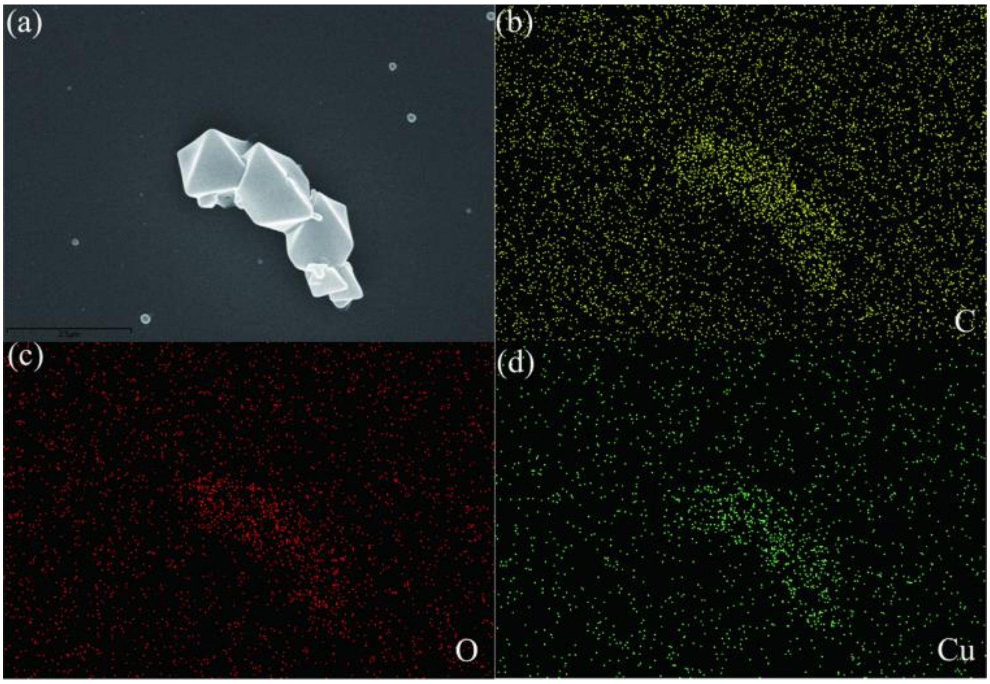

Figure SI5 the EDS of HKUST-1.

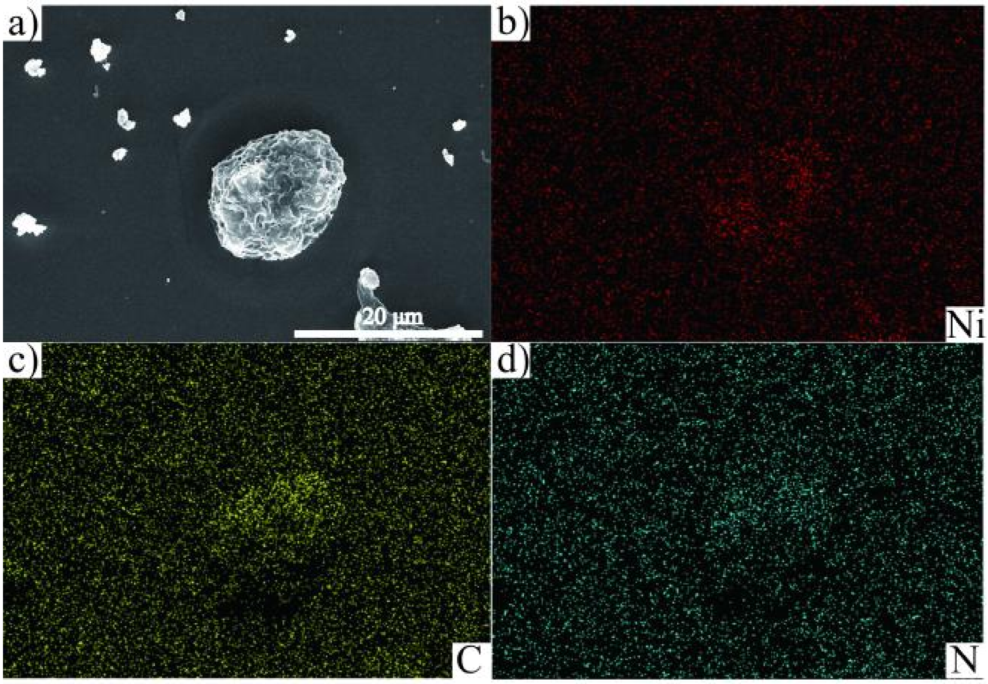

Figure SI6 the EDS of Ni-MOF.

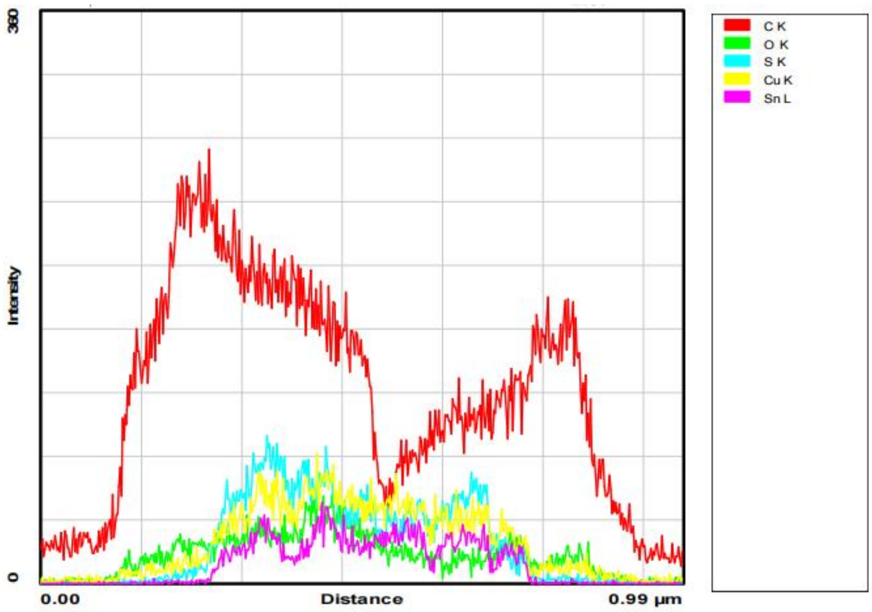

Figure SI7 The EDS line scanning profile of $SnSn_2$@HKUST-1.

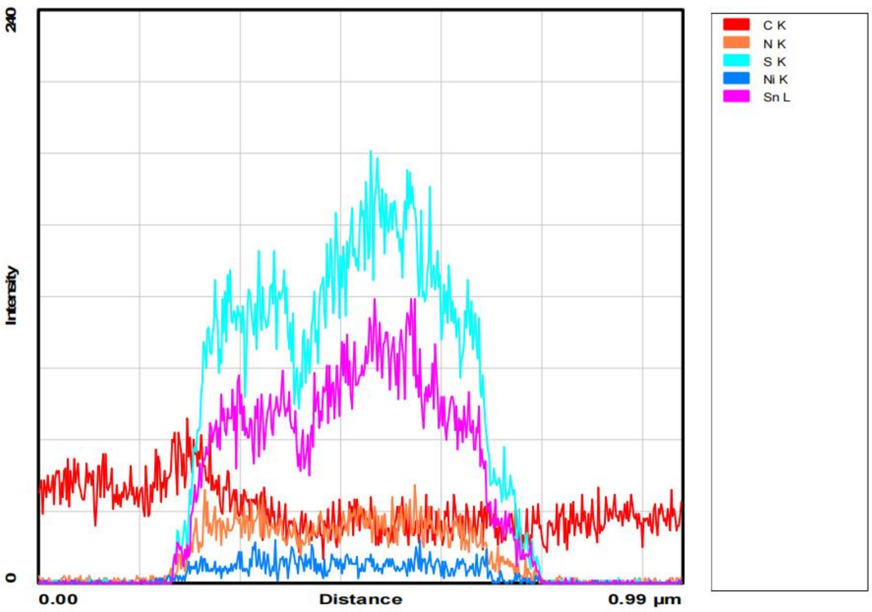

Figure SI8 The EDS line scanning profile of $SnSn_2$@Ni-MOF.

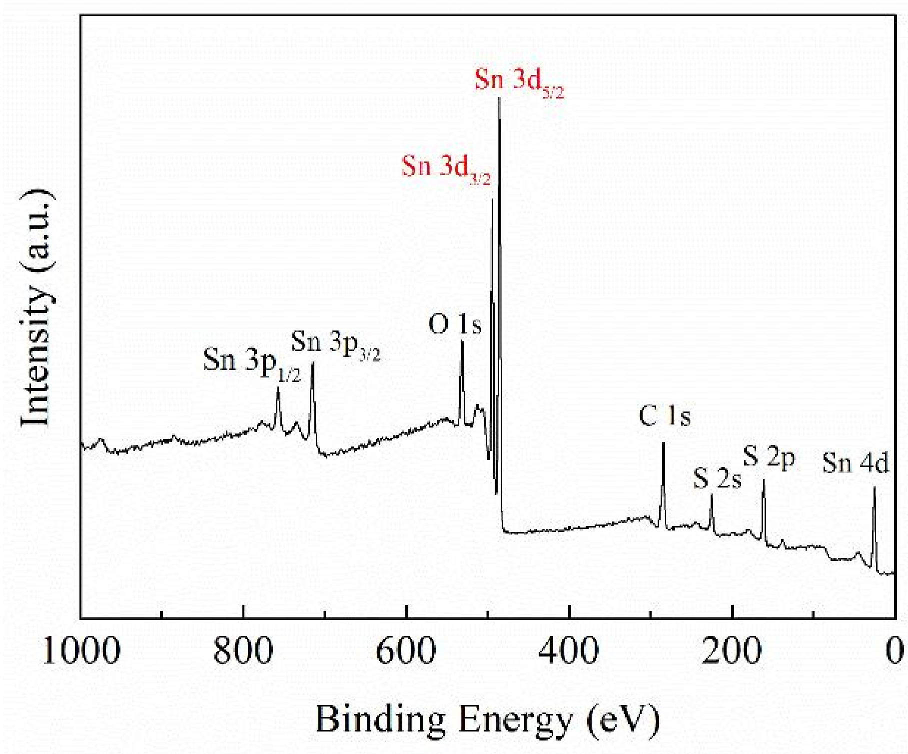

Figure SI9 The full scanning XPS spectrum of SnS_2.

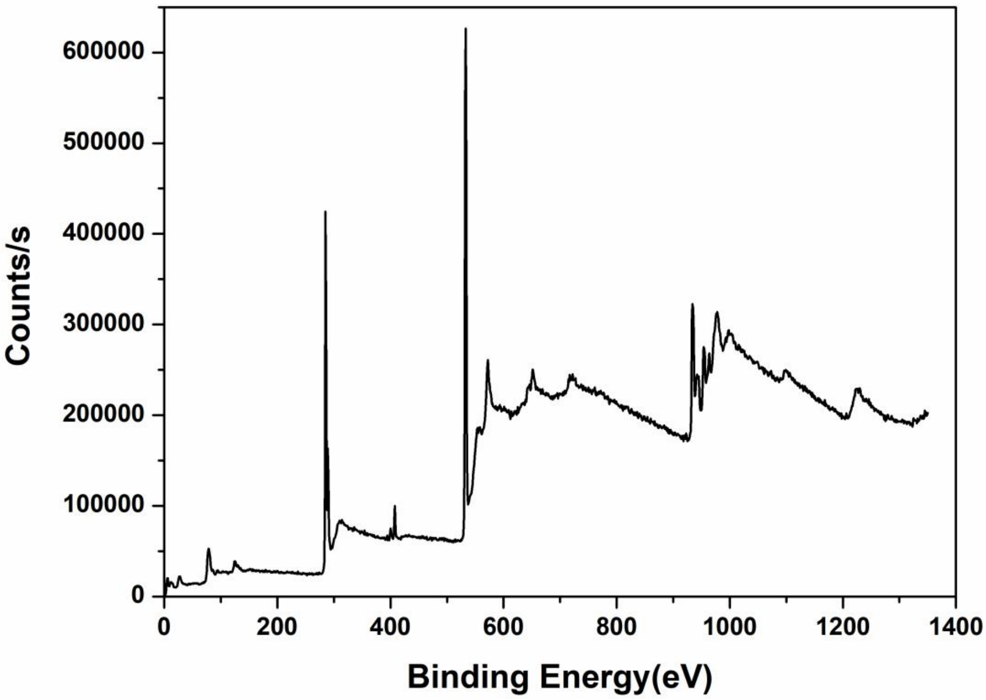

Figure SI10 The full scanning XPS spectrum of HKUST-1.

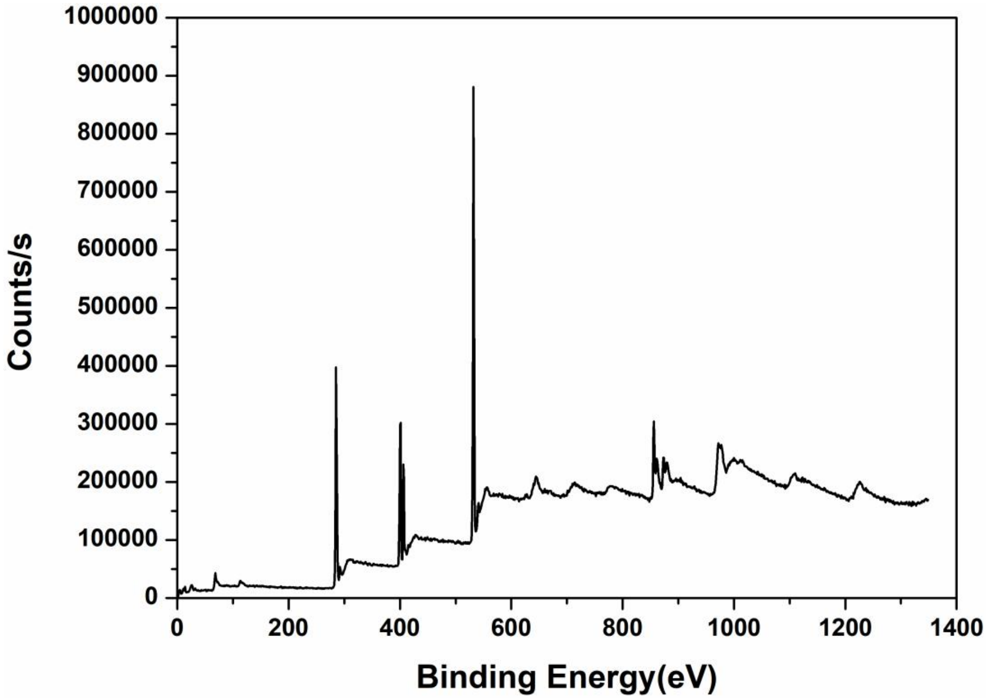

Figure SI11 The full scanning XPS spectrum of Ni-MOF.

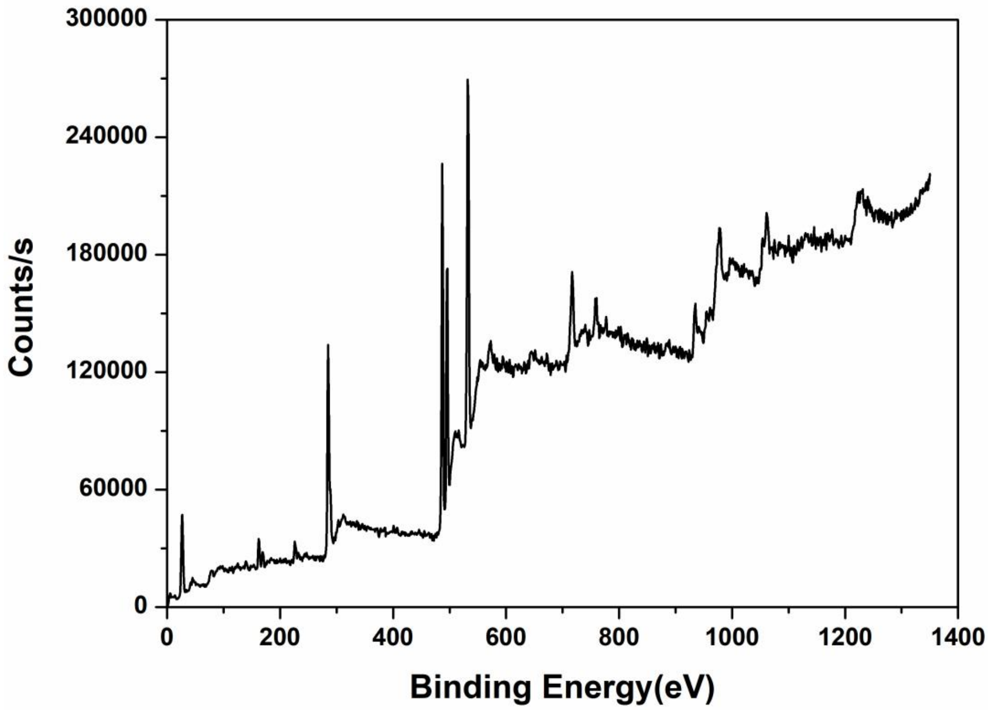

Figure SI12 The full scanning XPS spectrum of SnS_2@HKUST-1.

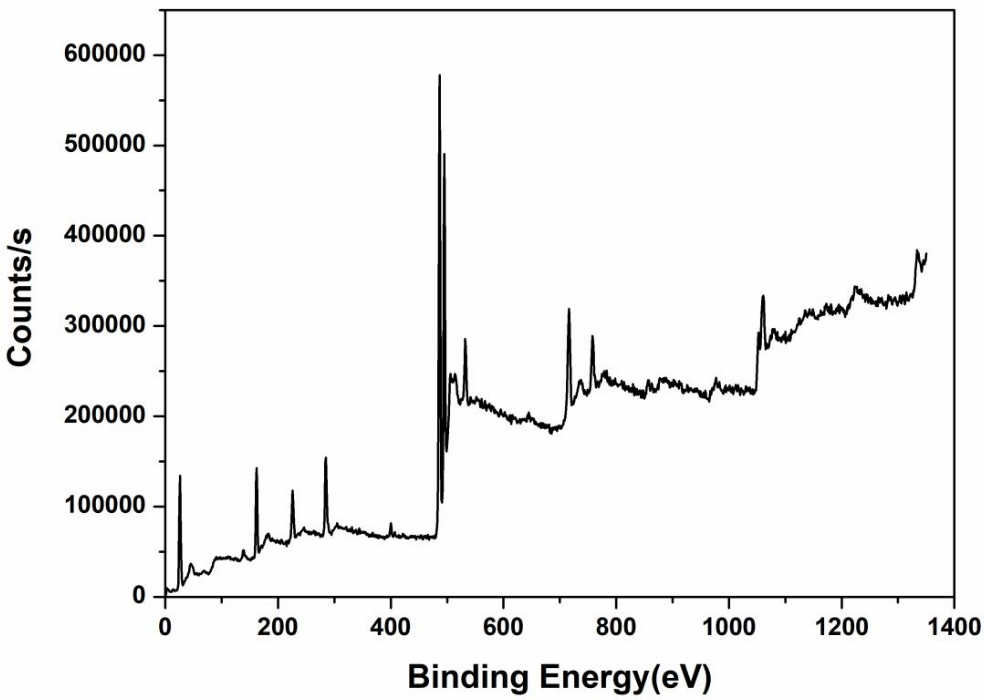

Figure SI13 The full scanning XPS spectrum of SnS_2@Ni-MOF.

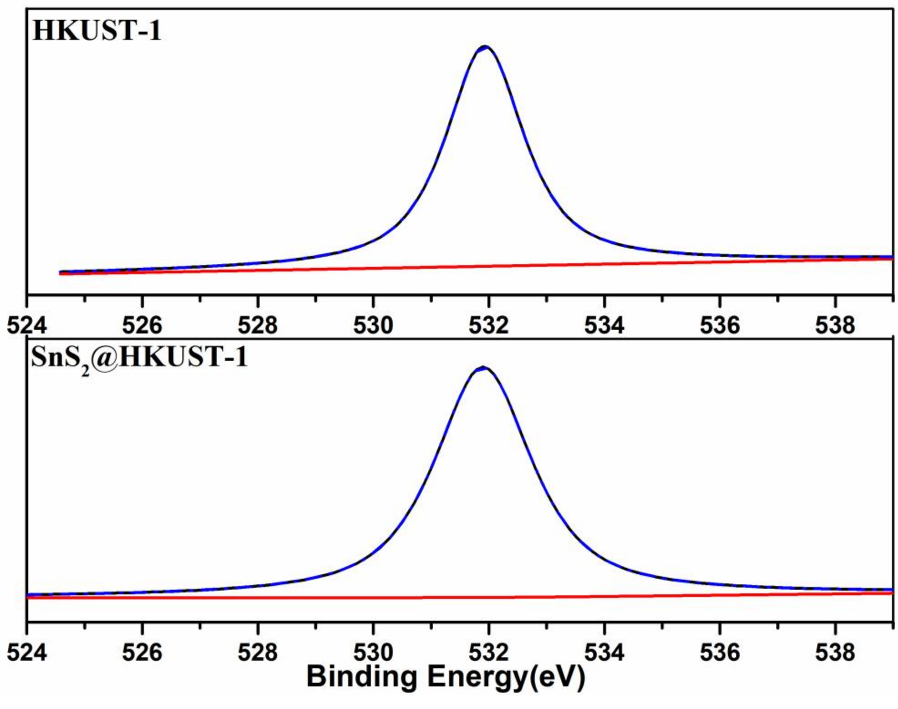

Figure SI14 The O 1s spectrum.

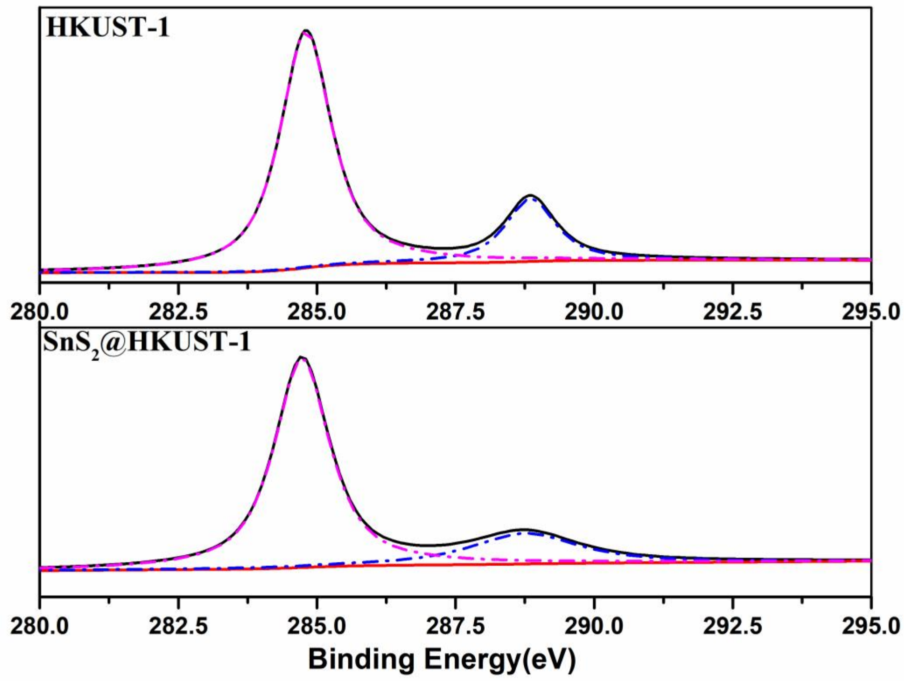

Figure SI15 The C 1s spectrum SnS_2@HKUST-1.

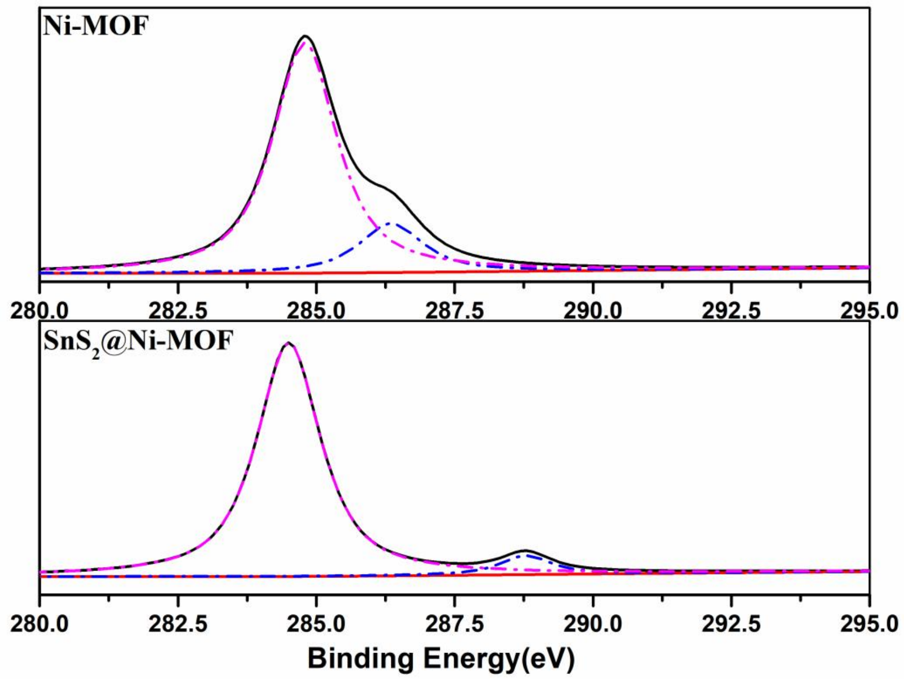

Figure SI16 The C 1s spectrum of SnS_2@Ni-MOF.

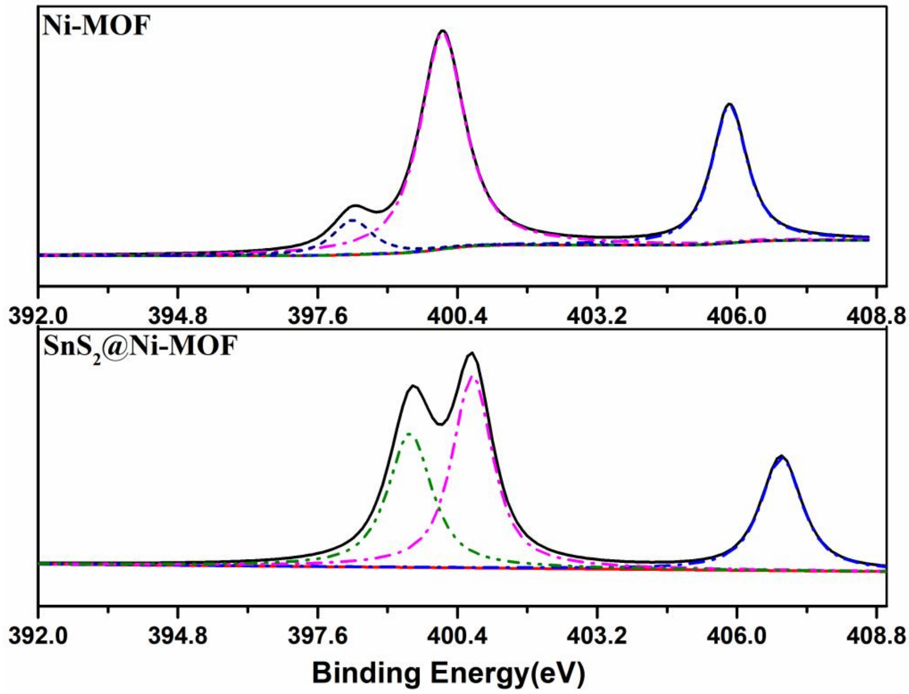

Figure SI17 The N 1s spectrum.

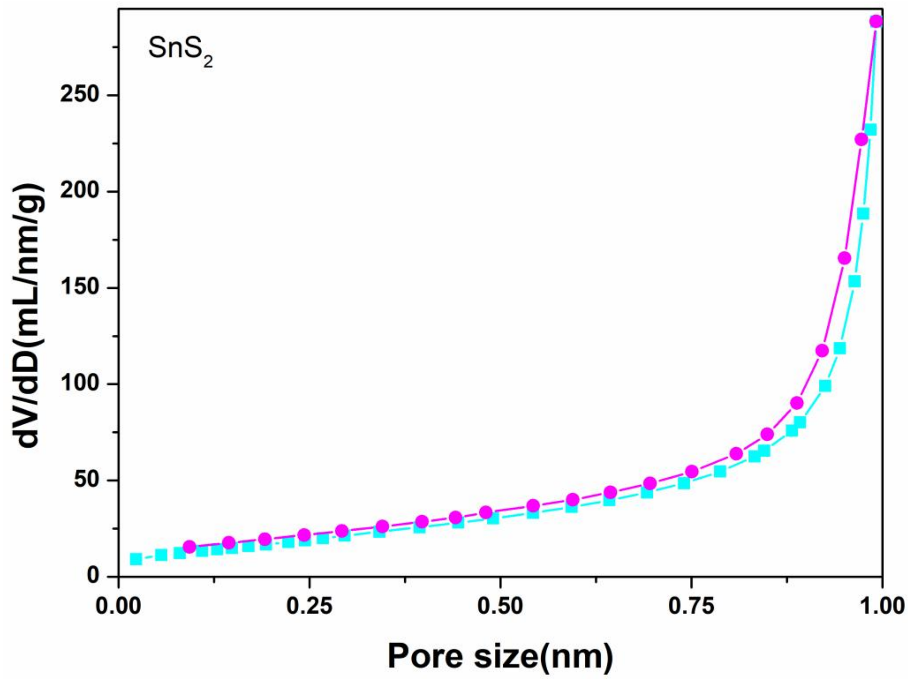

Figure SI18 The N_2 adsorption-desorption isotherm of SnS_2.

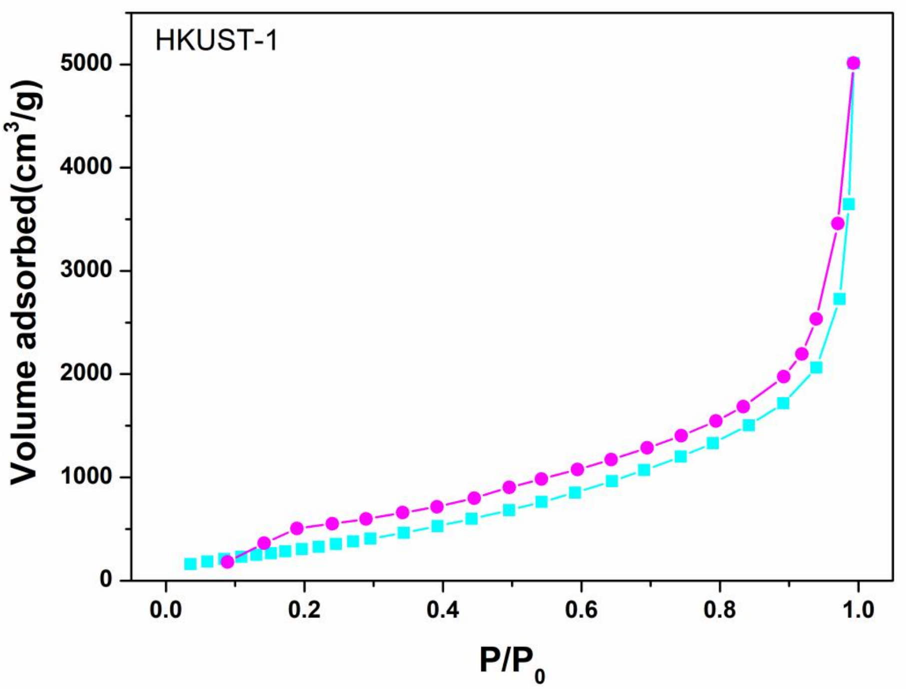

Figure SI19 The N_2 adsorption-desorption isotherm of HKUST-1.

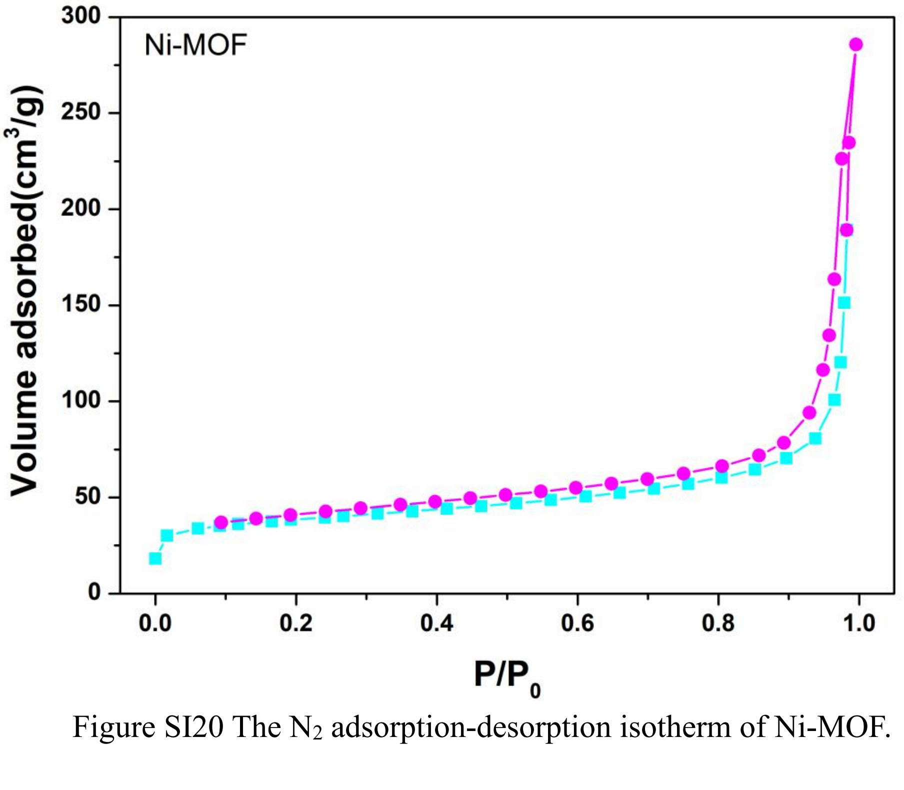

Figure SI20 The N_2 adsorption-desorption isotherm of Ni-MOF.

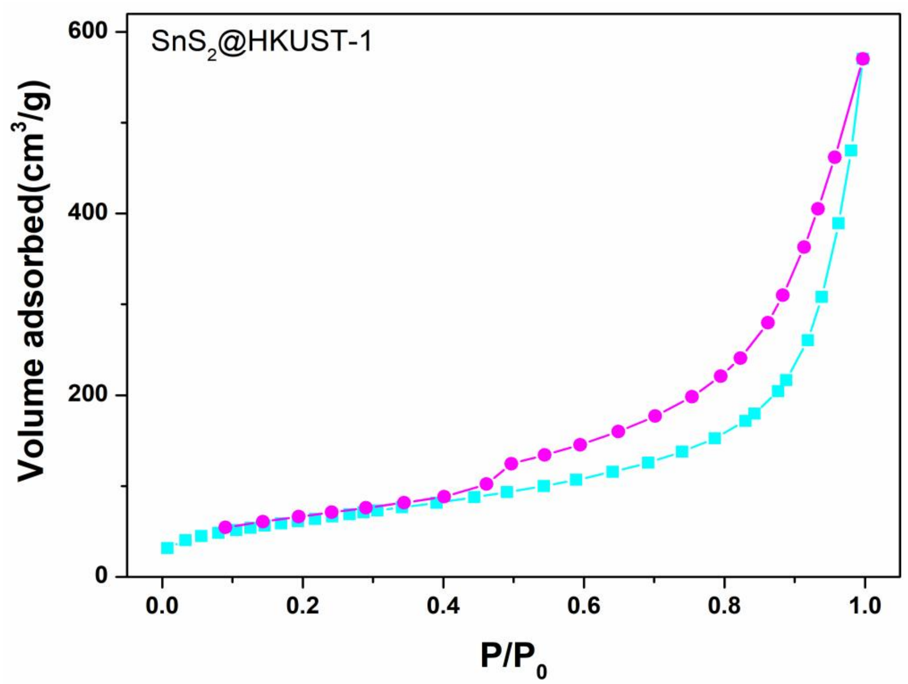

Figure SI21 The N_2 adsorption-desorption isotherm of SnS_2@HKUST-1.

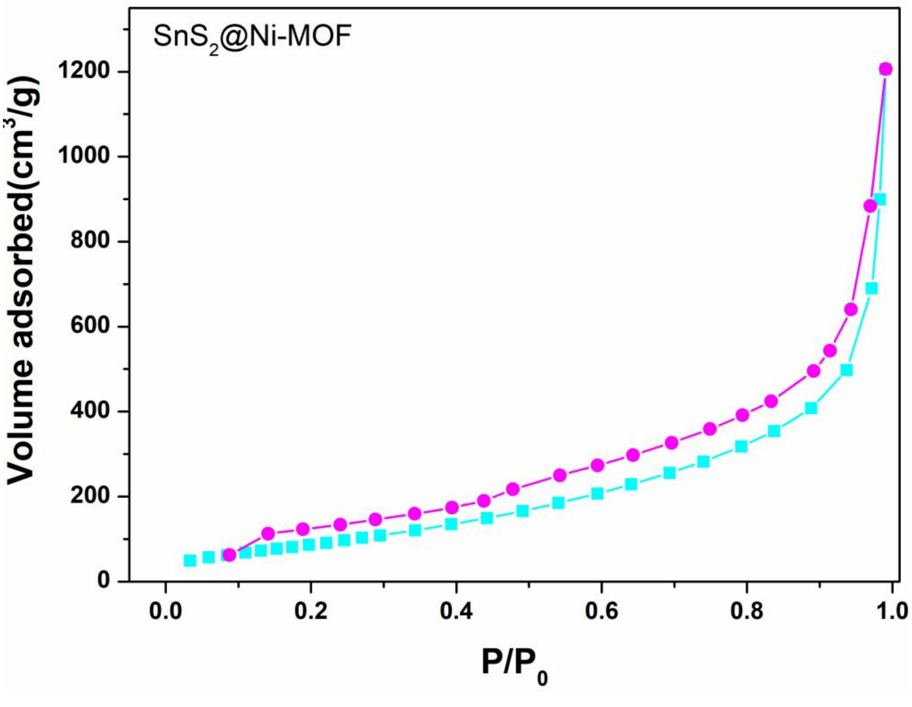

Figure SI22 The N_2 adsorption-desorption isotherm of SnS_2@Ni-MOF.

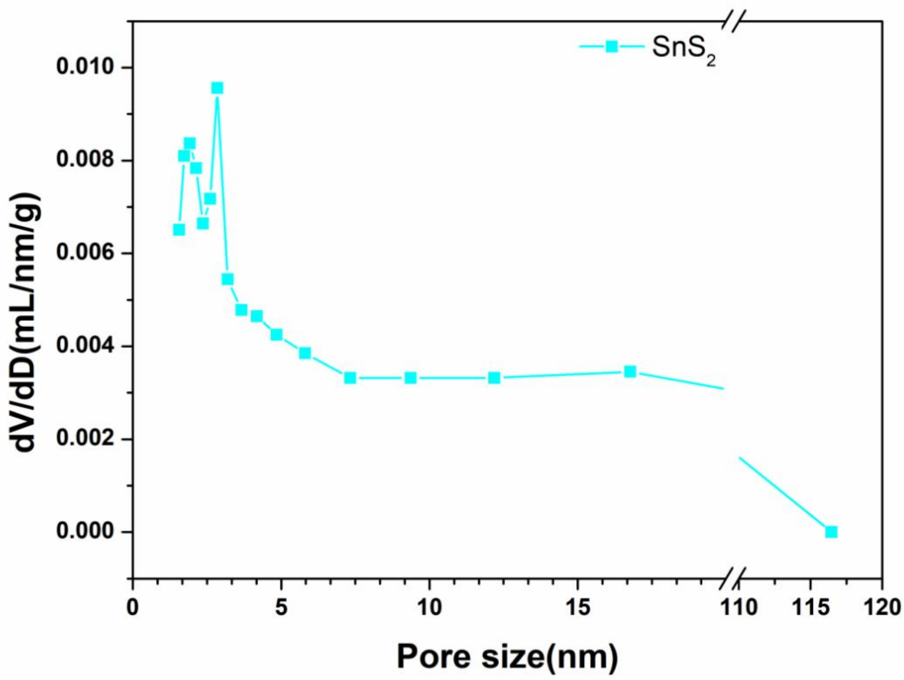

Figure SI23 The average pore sizes of SnS_2.

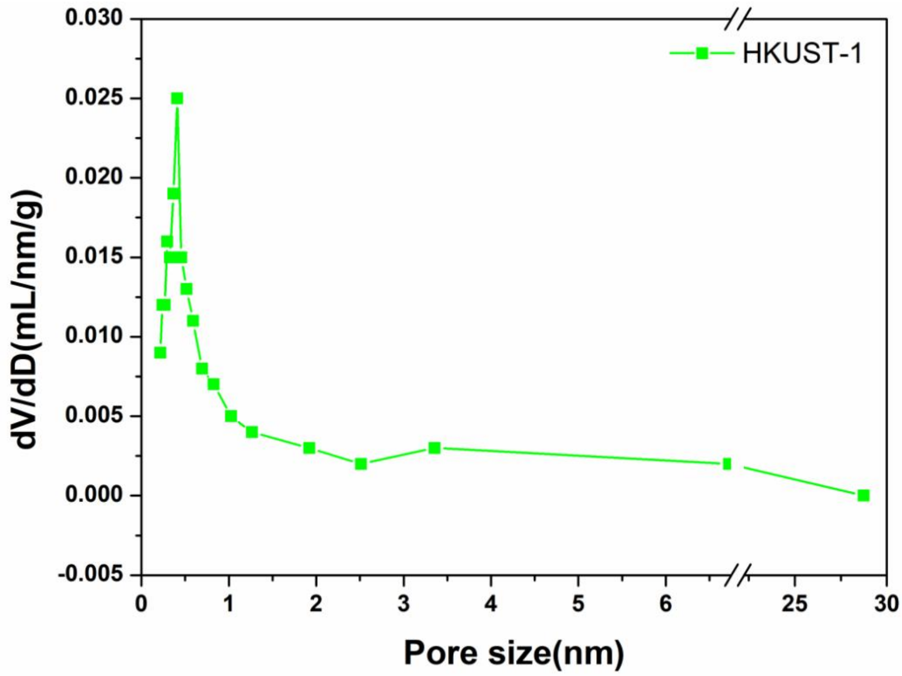

Figure SI24 The average pore sizes of HKUST-1.

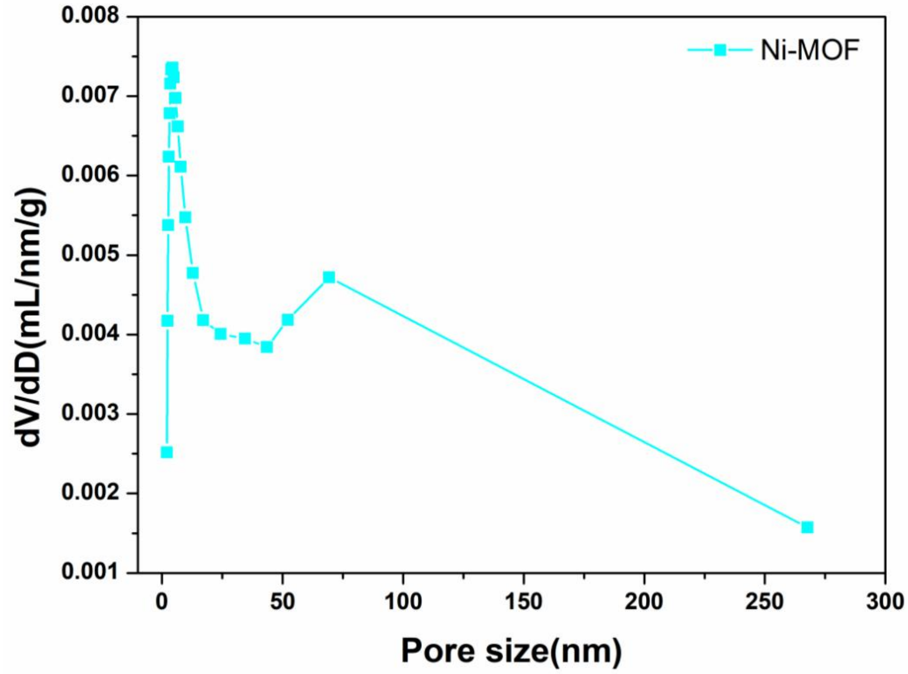

Figure SI25 The average pore sizes of Ni-MOF.

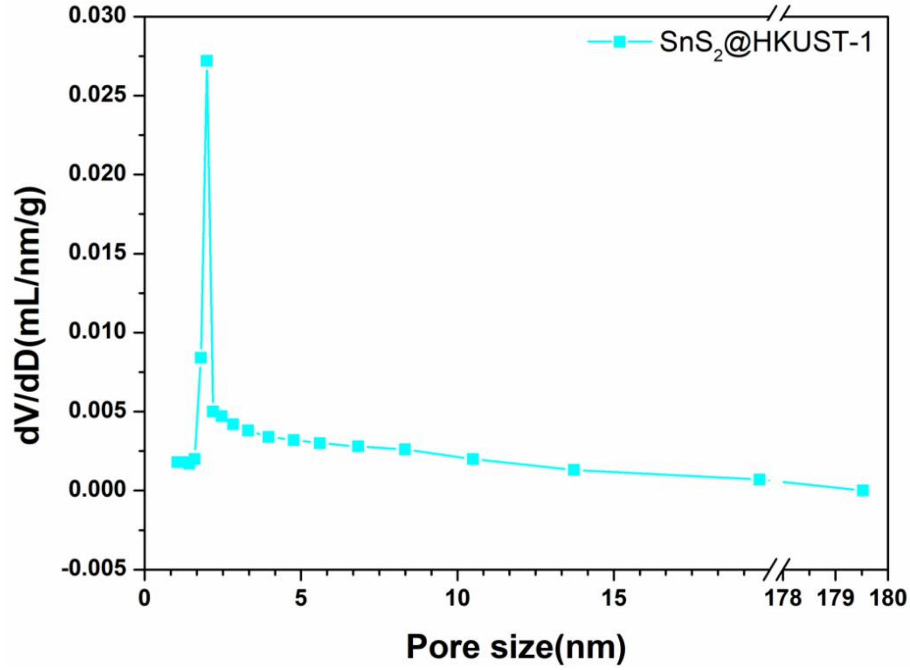

Figure SI26 The average pore sizes of SnS_2@HKUST-1.

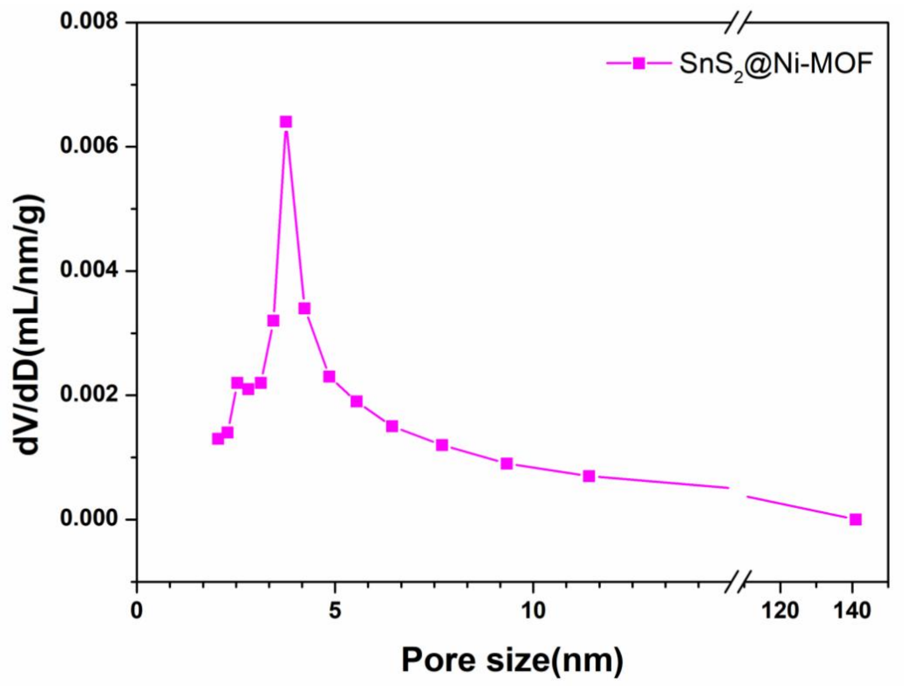

Figure SI27 The average pore sizes of SnS_2@Ni-MOF.

Table SI1 The LSV curves of the five different SnS_2 samples

Sample number	S1	S2	S4	S6	S8
Overpotential (mV)	262	272	292	202	181

Table SI2 The summary of catalysts for HER.

materials	**cycling stability**	**Electrolyte**	**Overpotential (mV)**	**Tafel slope (mV/dec)**	**Cdl (mF/cm^2)**	**Ref**
MoS_2NPs/SnS_2NS	negligible (500 cycles)	0.5M H_2SO_4	249mV	42.1 mV/dec	-	1
SnS_2	negligible (1000 cycles)	0.5M H_2SO_4	250mV	-	$0.226mF/cm^2$	2
MoS_2/SnS_2 heterojunction	Negligible (1000 cycles)	0.5M H_2SO_4	288mV	50 mV/dec	$7.82\ mF/cm^2$	3
SnS_2-1500C	Negligible (2000 cycles)	0.5M H_2SO_4	117mV	69 mV/dec	$16.79mF/cm^2$	4
CTS (S)	Negligible (2000 cycles)	0.5M H_2SO_4	230mV	76 mV/dec	$0.53mF/cm^2$	5
4% PANI/SnS_2	-	0.5M H_2SO_4	-	66 mV/dec	$0.85mF/cm^2$	6

Ni-Co-S-340(60)	-	1M KOH	129mV	96.1 mV/dec	23.3mF/cm^2	7
Ni-CNTs	-	0.5M H_2SO_4	261mV	88mV/dec	-	8
Ni@NC6-600	Negligible (1000 cycles)	1M KOH	181mV	119.3 mV/dec	10.4 mF/cm^2	9
Ni/Ni_3S_2@CN	Negligible (2000 cycles)	1M KOH	141mV	91 mV/dec	22.3 mF/cm^2	10
Ni-MOF/NC-800	Negligible (2000 cycles)	0.5M H_2SO_4	369mV	127.1 mV/dec	-	11
NPC-sheet@NF	-	1M KOH	97mV	64.8 mV/dec	33.6 mF/cm^2	12
Cu_3P@NiFe-MOF-4	-	1M KOH	175mV	131 mV/dec	-	13
$NiSe_2$-600@NC	Negligible (1000 cycles)	0.5M H_2SO_4	196mV	45 mV/dec	3.12 mF/cm^2	14
Co-MOF@Zn-800	Negligible (3000 cycles)	0.5M H_2SO_4	218mV	146.6 mV/dec	-	15
Pd/MOF	Negligible (1000 cycles)	0.5M H_2SO_4	105mV	85mV/dec	-	16
$Cu_{2-x}S$/CNFs	Negligible (2000 cycles)	1M KOH	276mV	59 mV/dec	29.3 mF/cm^2	17
Cu_3P/C-300	Negligible (2000 cycles)	1MKOH	233mV	91 mV/dec	0.7 mF/cm^2	18
10% Mo-SnS	negligible(3000 cycles)	0.5M H_2SO_4	377mV	100 mV/dec	-	19
SnS_2/G	-	1M KOH	360mV	257 mV/dec	0.9 mF/cm	20
Vs-SnS_2	-	0.5M H_2SO_4	141mV	74 mV/dec	-	21
Mn-SnS_2/NF	Negligible (2000 cycles)	1M KOH	71mV	72 mV/dec	26.72 mF/cm	22
$MoSe_2/SnS_2$	-	1M KOH	285mV	109 mV/dec	-	23
SnS_2-Pt-3	Negligible (1000 cycles)	0.5M H_2SO_4	210mV	126 mV/dec	6.3 mF/cm	24

Table SI3 The Tafel slope of the five different SnS_2 samples

Sample number	S1	S2	S4	S6	S8
Tafel slope (mV·dec^{-1})	113	103	110	104	106

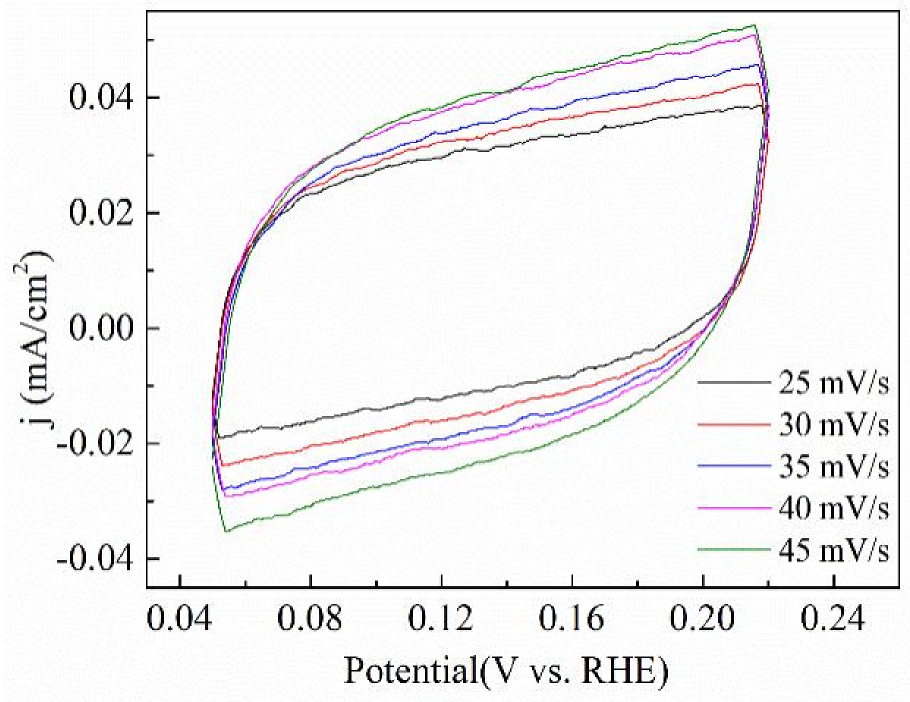

Figure SI28 The CV curves for **S1**.

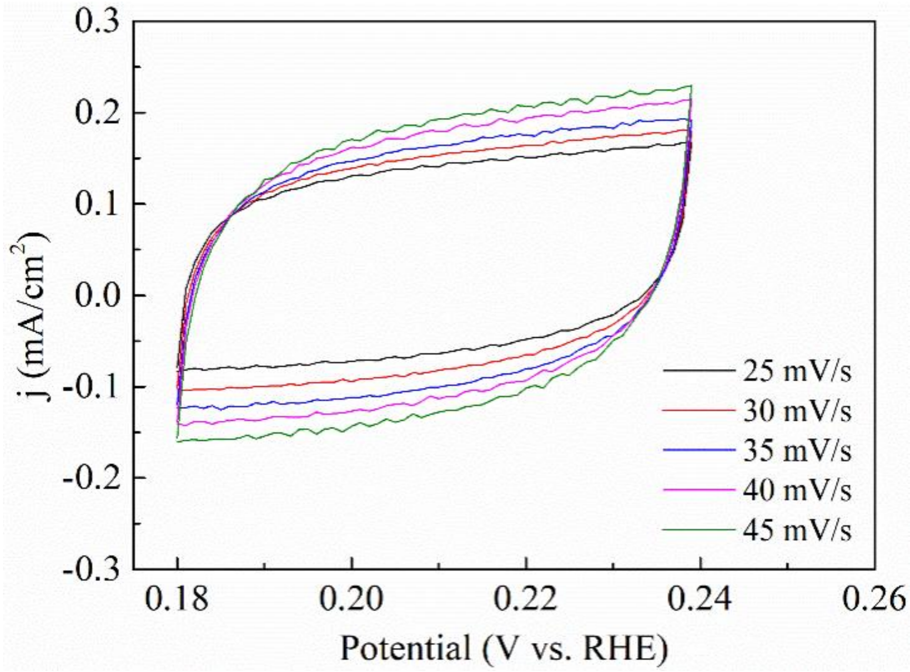

Figure SI29 The CV curves for **S2**.

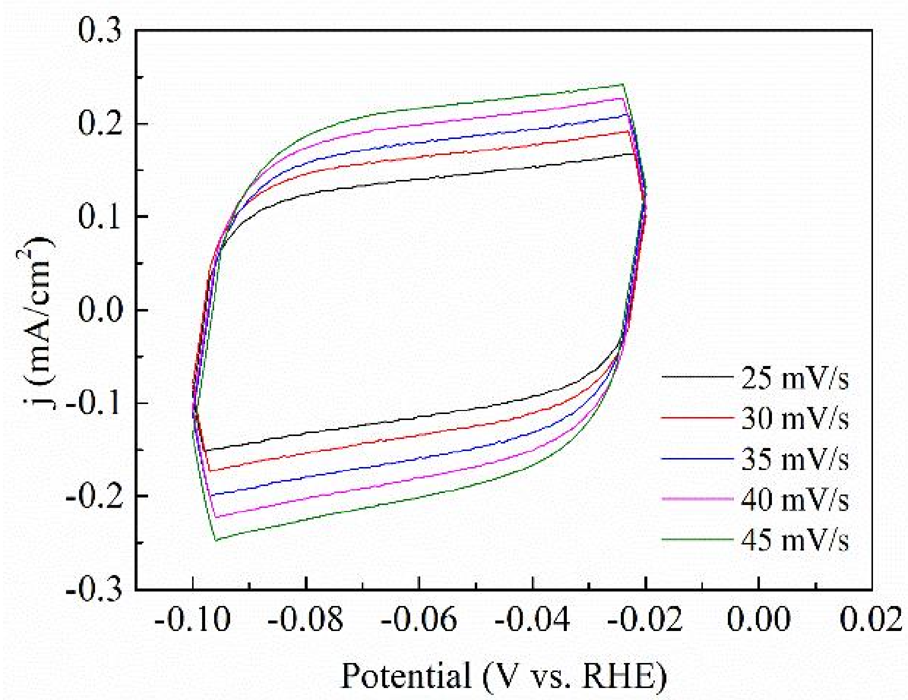

Figure SI30 The CV curves for **S4**.

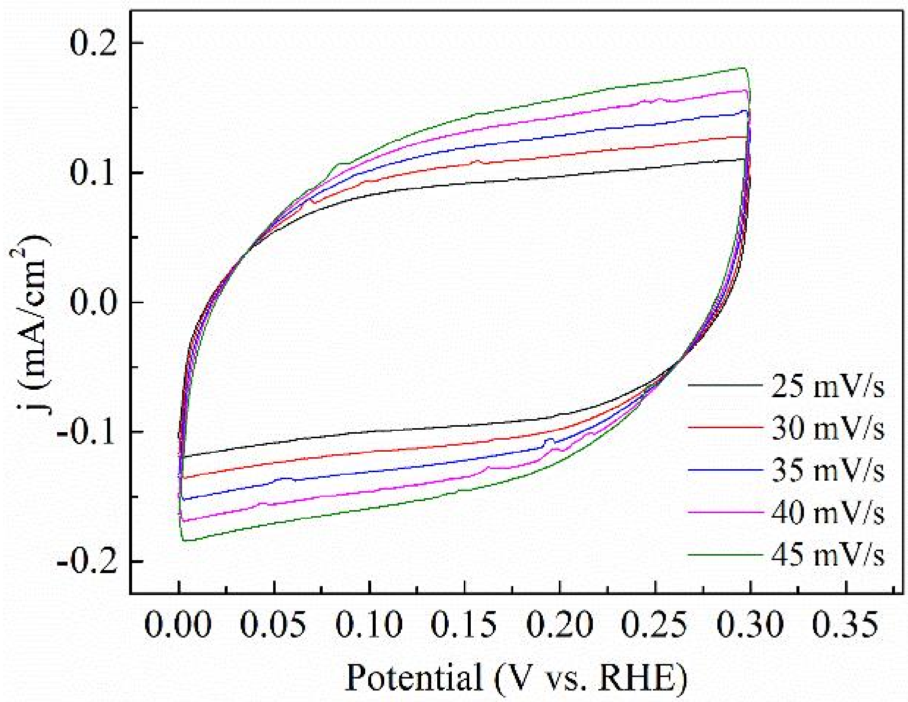

Figure SI31 The CV curves for **S6**.

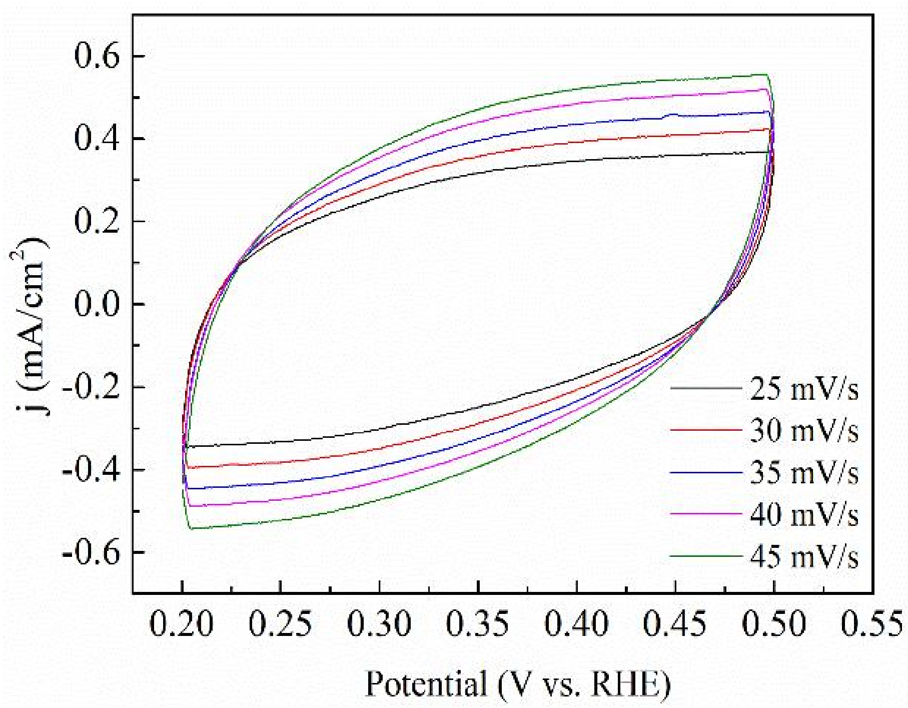

Figure SI32 The CV curves for **S8**.

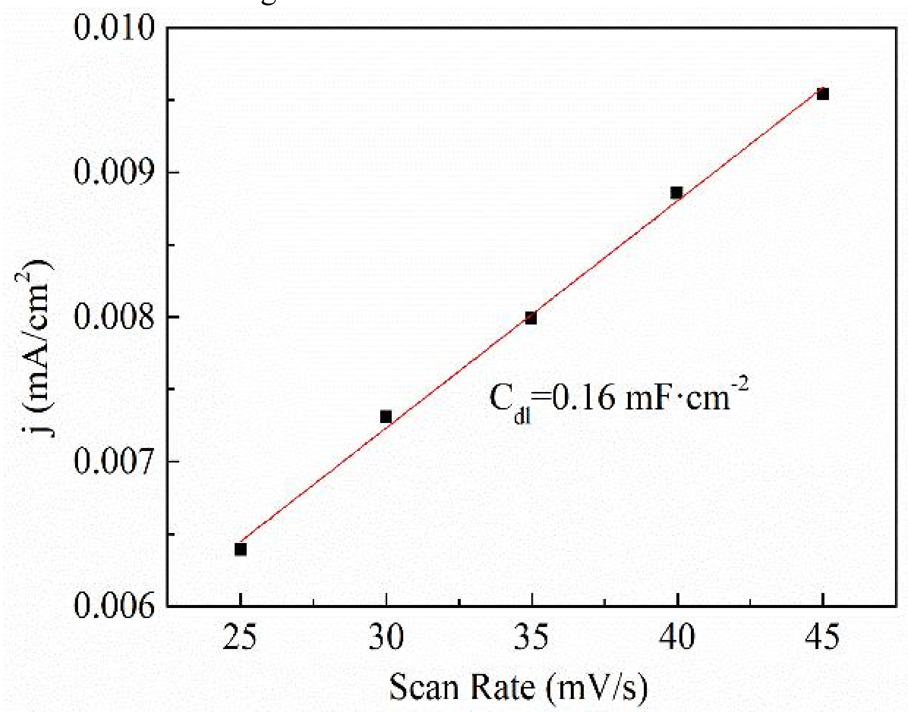

Figure SI33 The Cdl values for **S1**.

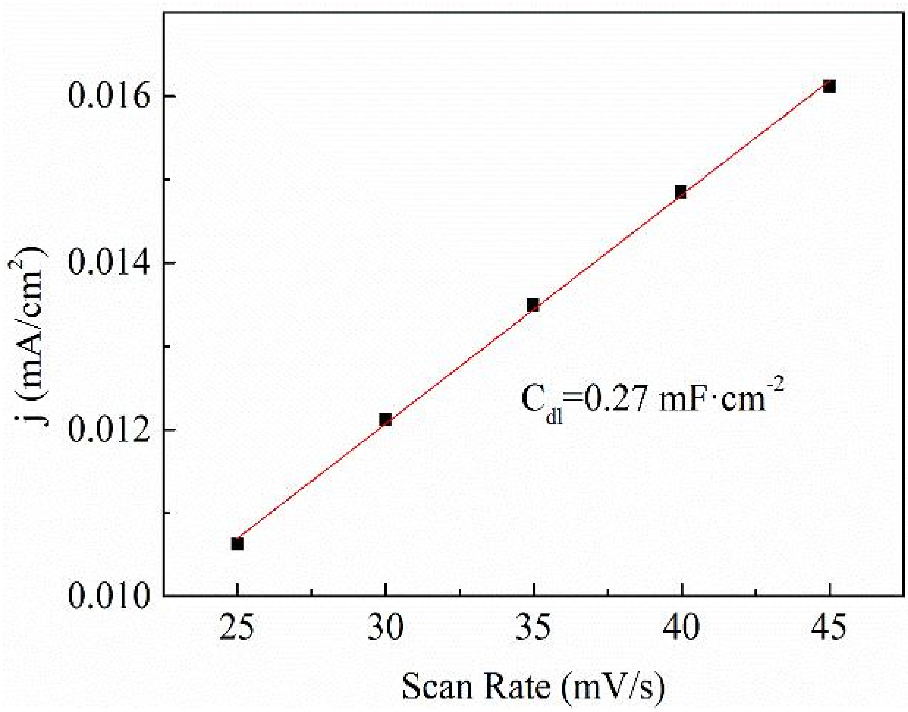

Figure SI34 The Cdl values for **S2**.

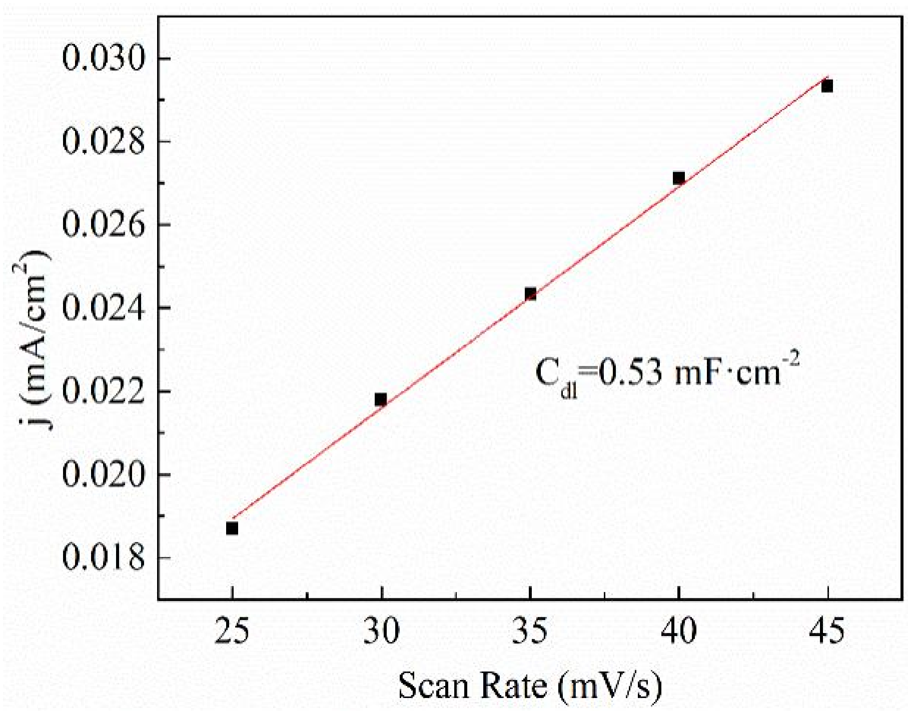

Figure SI35The Cdl values for **S4**.

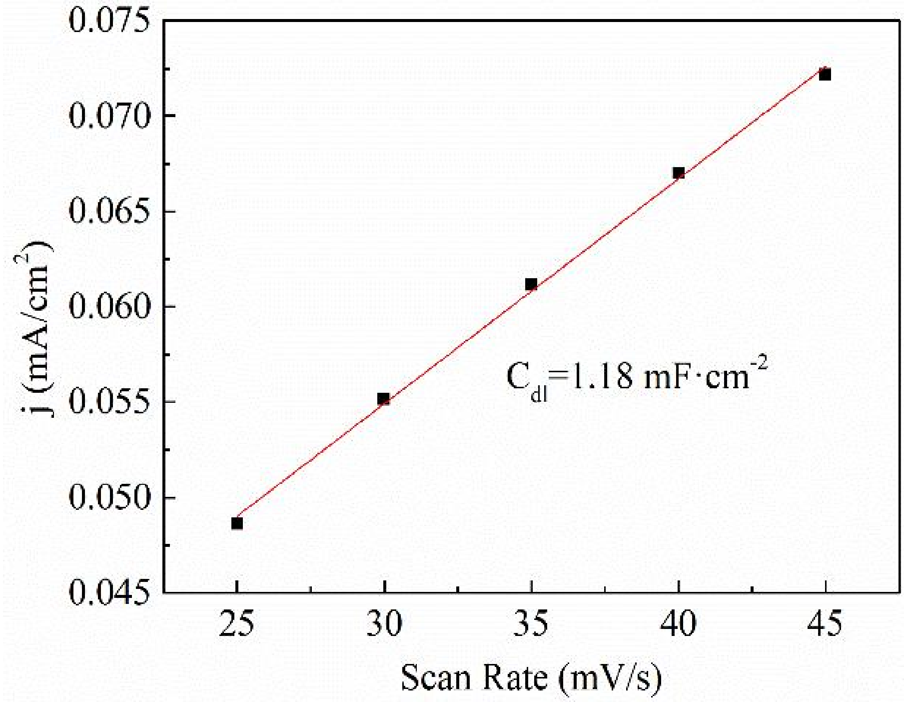

Figure SI36 The Cdl values for **S6**.

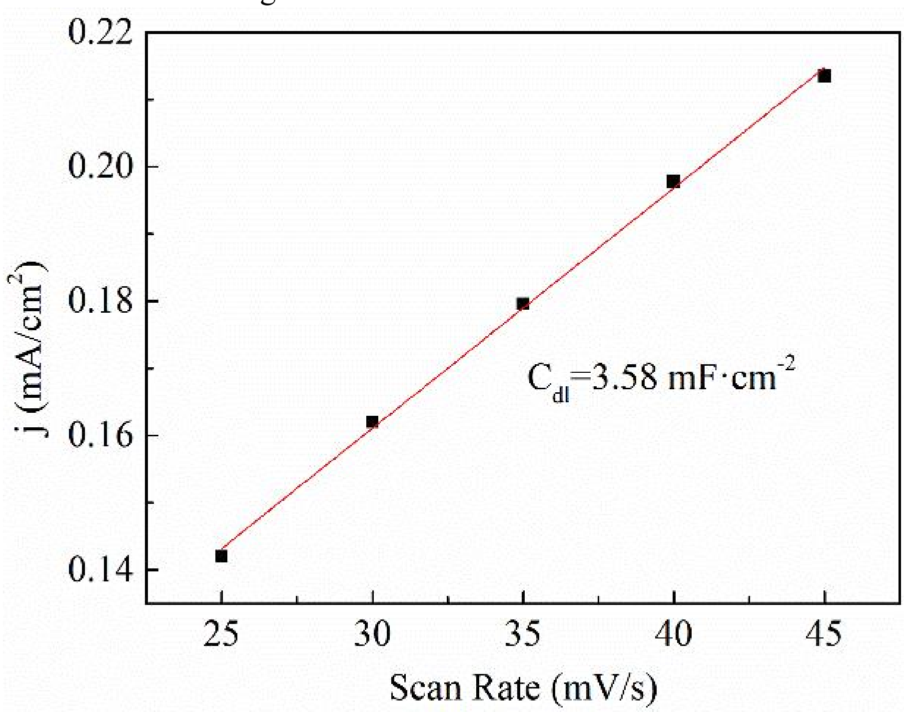

Figure SI37 The Cdl values for **S8**.

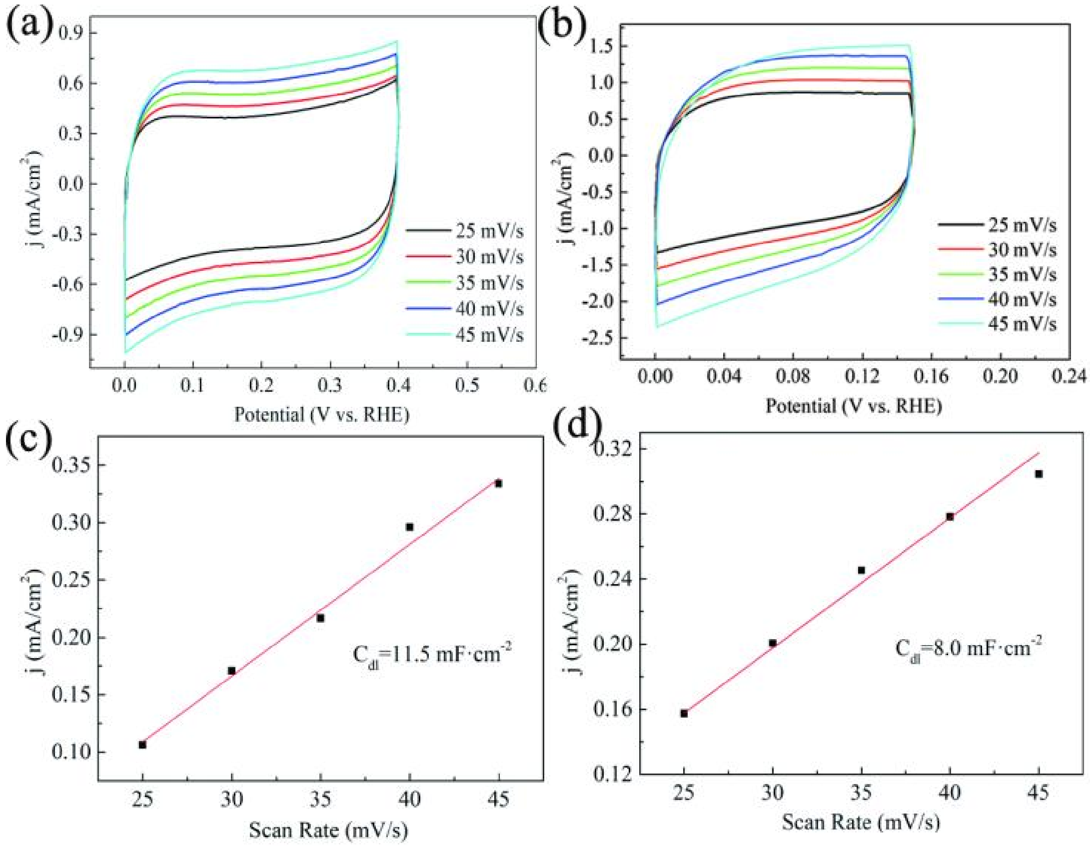

Figure SI38 (a) The CV curves of SnS2@Ni-MOF. (b) The CV curves of SnS2. @HKUST-1 (c) The Cdl values for SnS2@Ni-MOF. (d) The Cdl values for SnS2@HKUST-1.

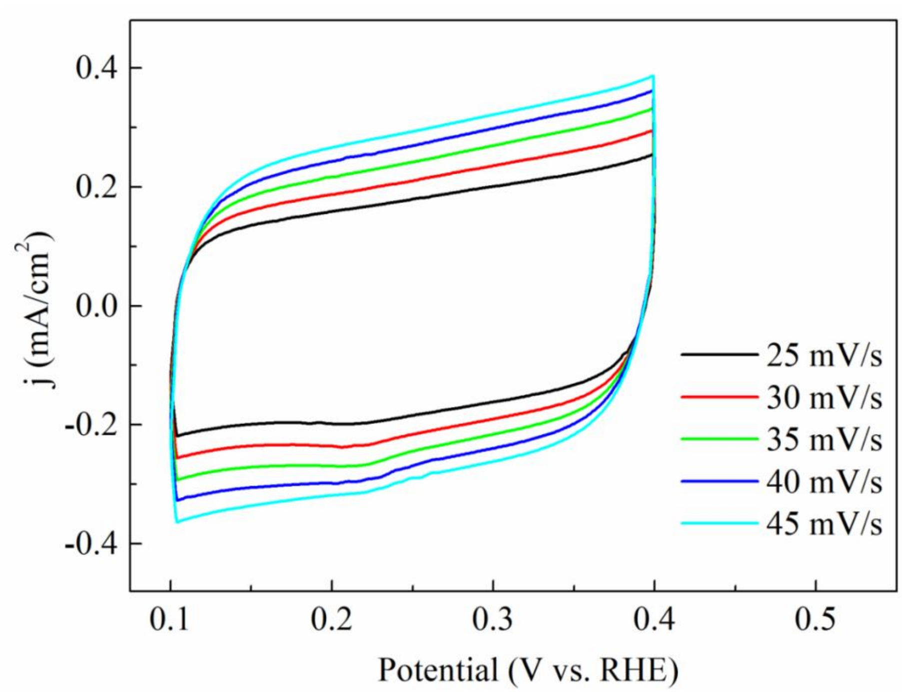

Figure SI39 The CV curves for Ni-MOF.

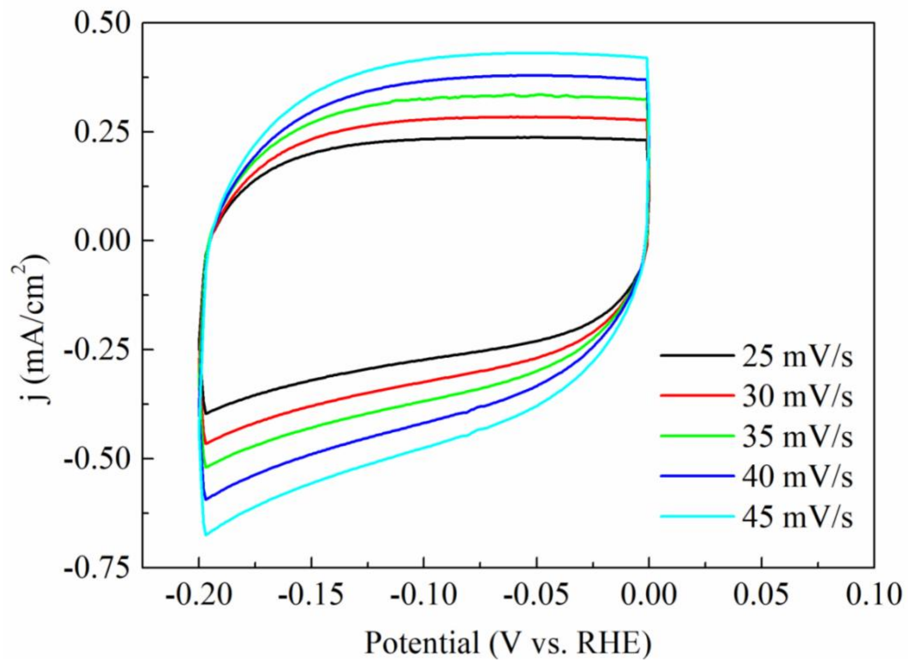

Figure SI40 The CV curves for HKUST-1.

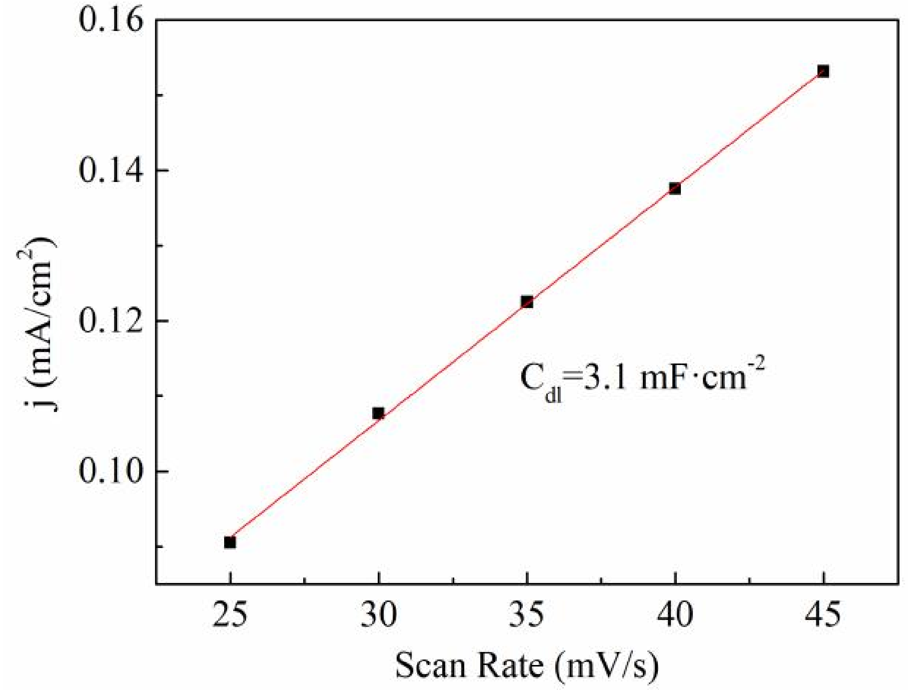

Figure SI41 The Cdl values for Ni-MOF.

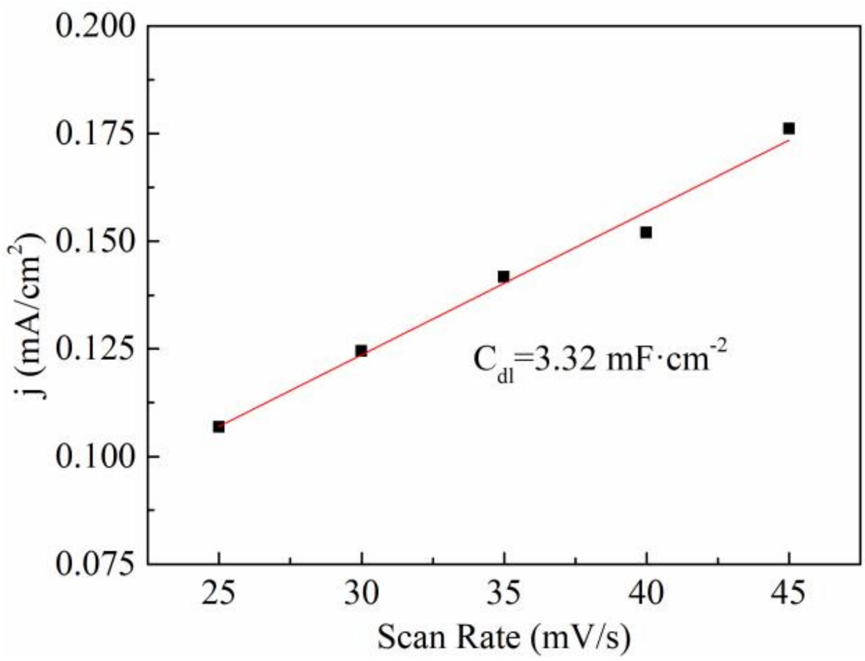

Figure SI42 The Cdl values for HKUST-1.

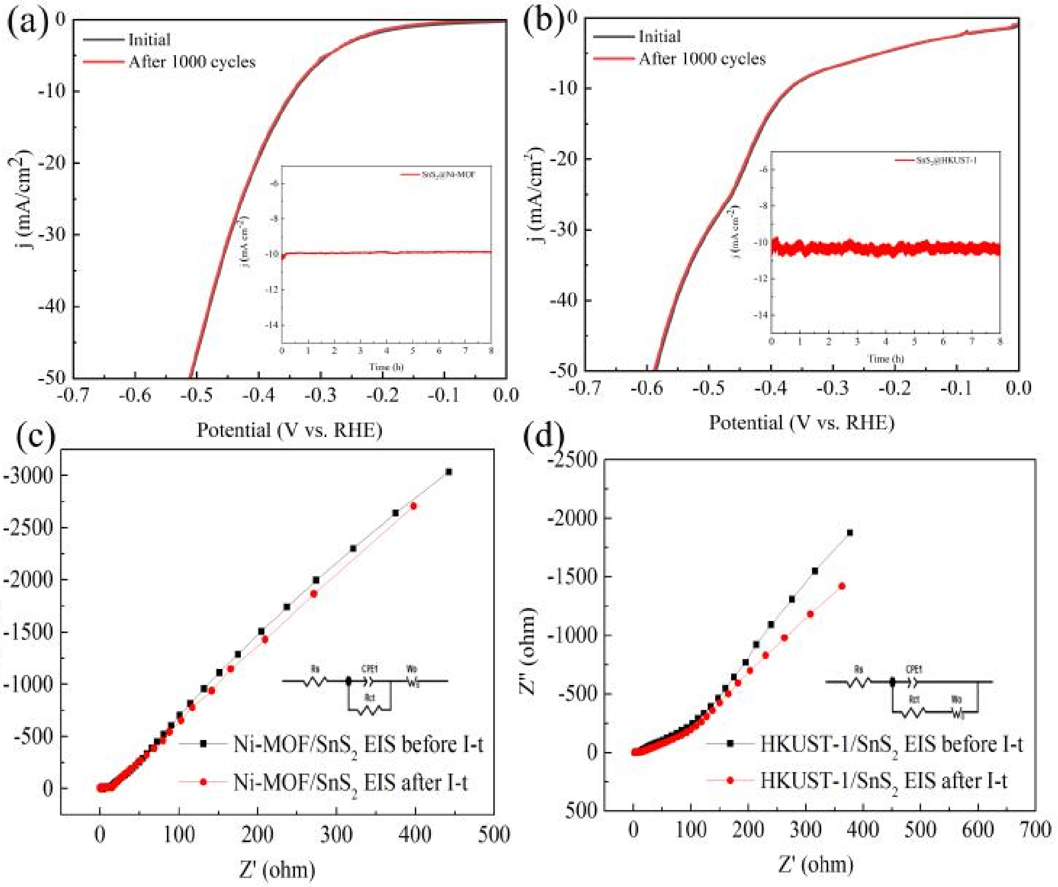

Figure SI43 (a) The polarization curves of SnS2@Ni-MOF before and after 1000 cycles; inset shows the chronopotentiometric curve @ 10 mA cm-2 for 8 h. (b) The polarization curves of SnS2@HKUST-1 before and after 1000 cycles; inset shows the chronopotentiometric curve @ 10 mA cm-2 for 8 h. (c) The SnS2@Ni-MOF EIS before and after I-t. (d) The SnS2@HKUST-1 EIS before and after I-t.

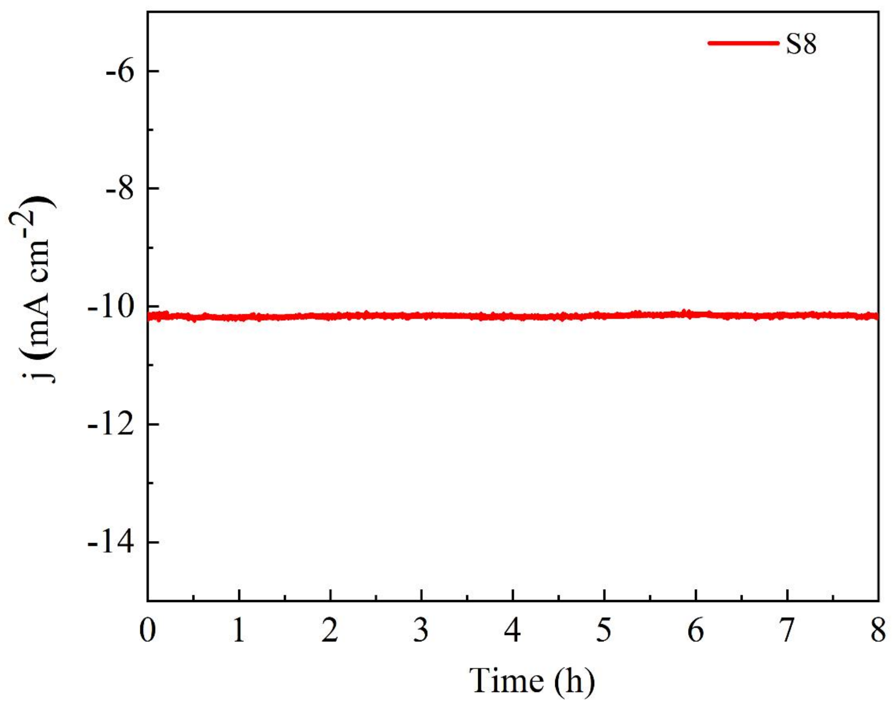

Figure SI44 The stability of SnS_2 (**S8**).

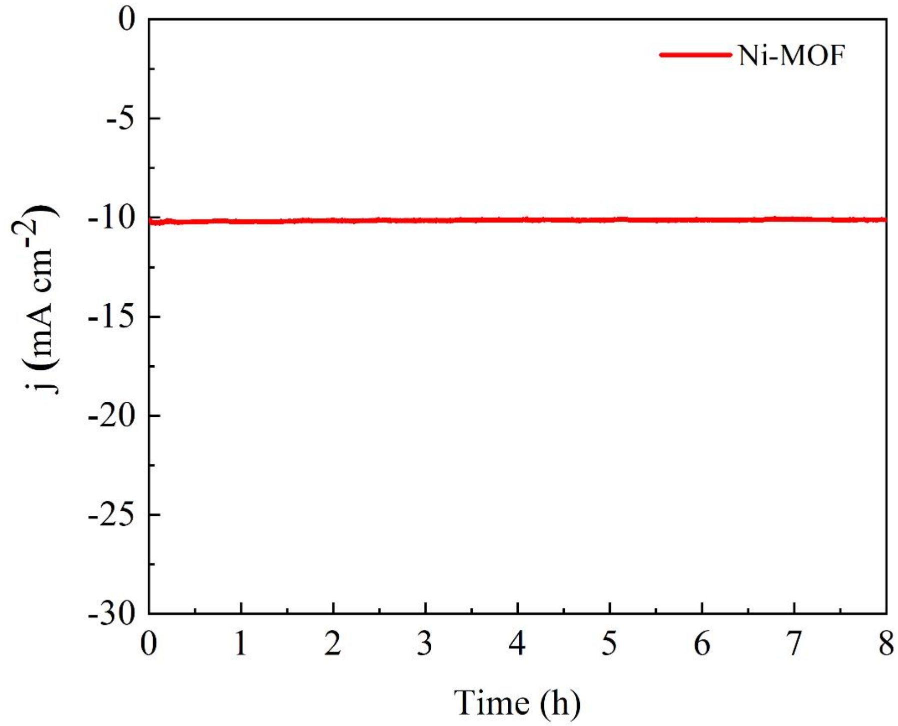

Figure SI45 The stability of Ni-MOF.

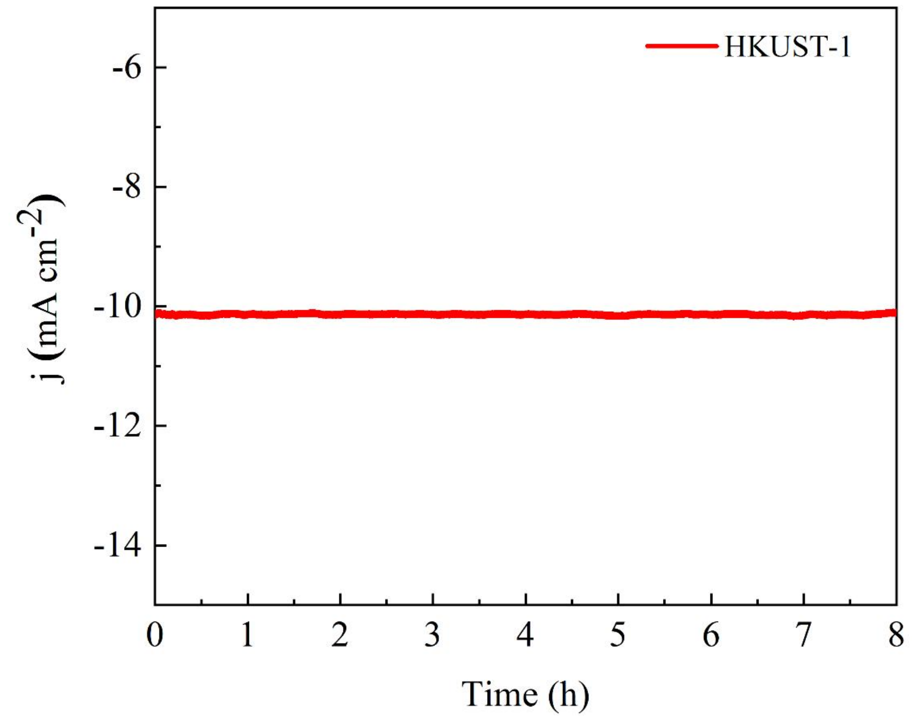

Figure SI46 The stability of HKUST-1.

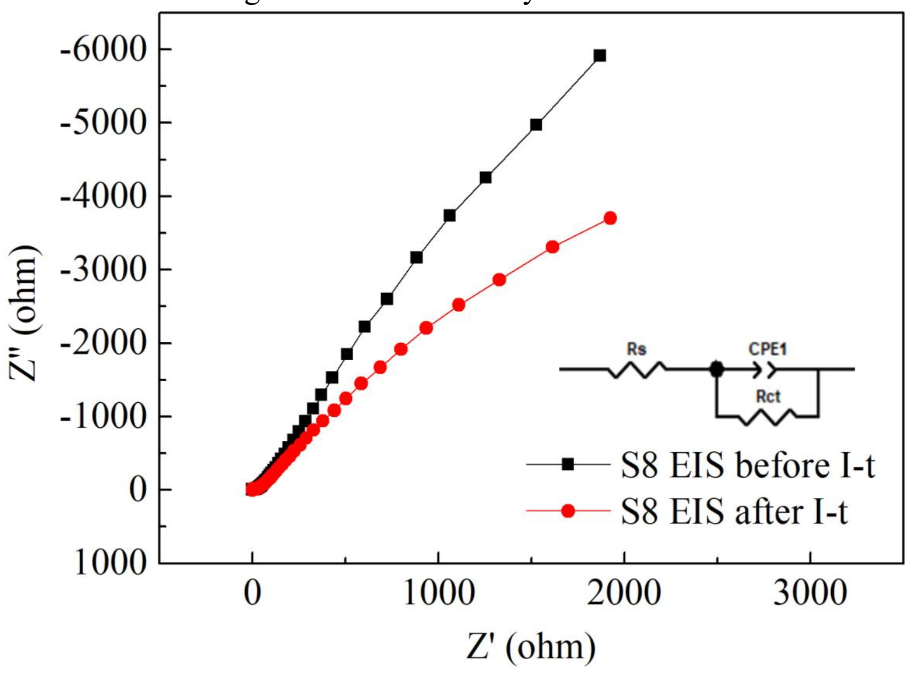

Figure SI47 The SnS_2 EIS before and after I-t.

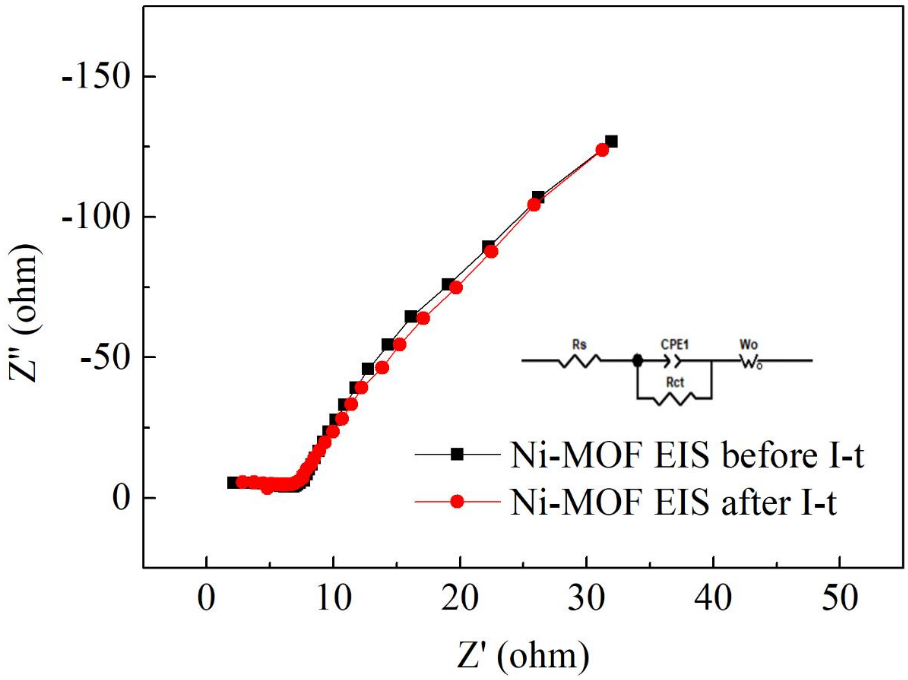

Figure SI48 The Ni-MOF EIS before and after I-t.

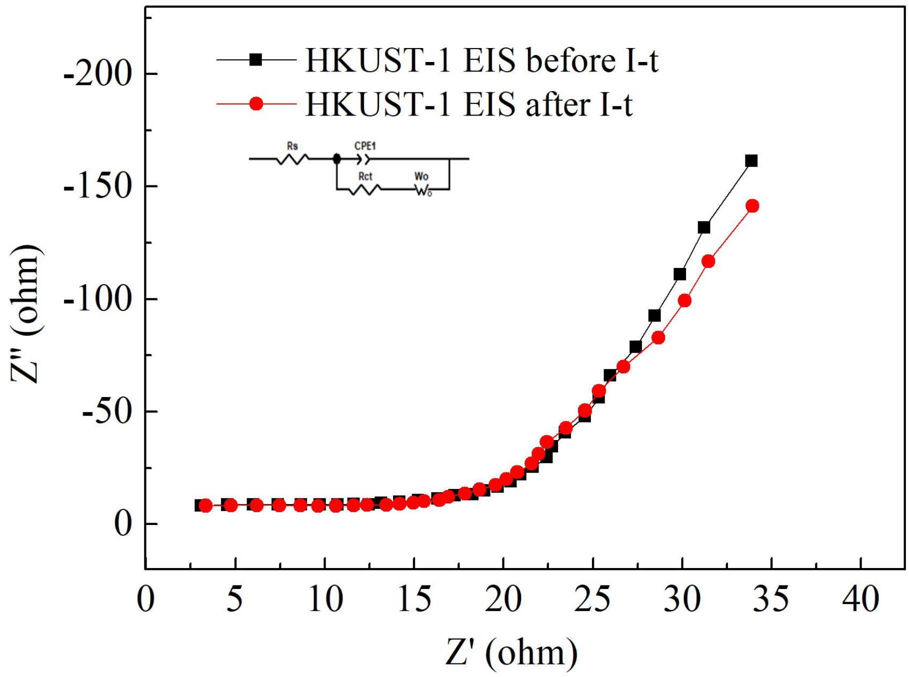

Figure SI49 The HKUST-1 EIS before and after I-t.

Table SI4 ICP-MS determination results Concentration of S, Sn and Ni in electrolyte solution after electrochemical test.

sample	Value type	S	Sn	Ni
Ni-MOF	Reported	15726 mg/L	/	/
SnS_2@Ni-MOF	Reported	15292mg/L	/	/

References

[1] L. Hu, X.-F. Song, S.-L. Zhang, H.-B. Zeng, X.-J. Zhang, R. Marks and D. Shan, Journal of Catalysis, 2018, 366, 8-15.

[2] H. Song, H. Wu, Y. Gao, K. Wang, X. Su, S. Yan and Y. Shi, Journal, 2019, 9.

[3] X. Xiao, Y. Wang, X. Xu, T. Yang and D. Zhang, Molecular Catalysis, 2020, 487, 110890.

[4] G. Liu, Y. Qiu, Z. Wang, J. Zhang, X. Chen, M. Dai, D. Jia, Y. Zhou, Z. Li and P. Hu, ACS Applied Materials & Interfaces, 2017, 9, 37750-37759.

[5] V. Maheskumar, P. Gnanaprakasam, T. Selvaraju and B. Vidhya, Journal of Electroanalytical Chemistry, 2018, 826, 38-45.

[6] Y. Zhang, L. Hu, H. Zhou, H. Wang and Y. Zhang, ACS Applied Nano Materials, 2022, 5, 391-400.

[7] C. Wu, Y. Du, Y. Fu, W. Wang, T. Zhan, Y. Liu, Y. Yang and L. Wang, Composites Part B: Engineering, 2019, 177, 107252.

[8] B. Thangavel, S. Berchmans and G. Venkatachalam, Energy & Fuels, 2021, 35, 1866-1873.

[9] N. Cheng, N. Wang, L. Ren, G. Casillas-Garcia, N. Liu, Y. Liu, X. Xu, W. Hao, S. X. Dou and Y. Du, Carbon, 2020, 163, 178-185.

[10] J. Tian, Y. Xu, J. Li, J. Chi, L. Feng, Q. Pan, X. Li and Z. Su, Journal of Solid State Chemistry, 2022, 313, 123287.

[11] J.-L. Liu, X.-Y. Zhou, L. Qin, Y.-Q. Wang, H.-J. Zhu, G. Ni, M.-L. Ma and M.-D. Zhang, Journal of Molecular Structure, 2022, 1252, 132184.

[12] H. Qu, Y. Ma, Z. Gou, B. Li, Y. Liu, Z. Zhang and L. Wang, Journal of Colloid and Interface Science, 2020, 572, 83-90.

[13] E. Li, Q. Mou, Z. Xu, J. Ma, X. Liu, G. Cheng, P. Zhao and H. Li, Catalysis Letters, 2022, 152, 3825-3832.

[14] N. Sahu, J. K. Das and J. N. Behera, Inorganic Chemistry, 2022, 61, 2835-2845.

[15] L. Qin, J.-L. Liu, X.-Y. Zhou, Y.-Q. Wang, X. Sun and M.-D. Zhang, Energy & Fuels, 2022, 36, 5843-5851.

[16] M. Nie, H. Sun, D. Lei, S. Kang, J. Liao, P. Guo, Z. Xue and F. Xue, Materials Chemistry and Physics, 2020, 254, 123481.

[17] Y. Bai, Y. Li, G. Liu and J. Hu, Journal, 2021, 11.

[18] B. Ren, Q. Yi, F. Yang, Y. Cheng, H. Yu, P. Han, Y. Yang, G. Chen, I. Jeerapan, Z. Li and J. Z. Ou, Energy & Fuels, 2022, 36, 8381-8390.

[19] S. R. Kadam, S. Ghosh, R. Bar-Ziv and M. Bar-Sadan, Chemistry – A European Journal, 2020, 26, 6679-6685.

[20] S. P. Lonkar, V. V. Pillai, S. P. Patole and S. M. Alhassan, ACS Applied Energy Materials, 2020, 3, 4995-5005.

[21] G. Shao, H. Xiang, M. Huang, Y. Zong, J. Luo, Y. Feng, X.-X. Xue, J. Xu, S. Liu and Z. Zhou, Science China Materials, 2022, 65, 1833-1841.

[22] Q. Zhai, H. Ji, Y. Ren, H. Wu, B. Wang, F. Li, Y. Ma and X. Meng, International Journal of Hydrogen Energy, 2022, 47, 21942-21951.

[23] Y. Chen, X. Wang, M. Lao, K. Rui, X. Zheng, H. Yu, J. Ma, S. X. Dou and W.

Sun, Nano Energy, 2019, 64, 103918.
[24] Y. Yu, J. Xu, J. Zhang, F. Li, J. Fu, C. Li and C. An, Journal, 2020, 10.